PARTIAL INHIBITION OF MITOCHONDRIAL COMPLEX I ACTIVATES STRESS RESPONSE PATHWAYS INDUCING A PROTECTION AGAINST OXIDATIVE STRESS

A Thesis

by

UTKARSH TRIPATHI

Submitted to the Office of Graduate and Professional Studies of
Texas A&M University
in partial fulfillment of the requirements for the degree of

MASTER OF SCIENCE

Chair of Committee,	Paul Lindahl
Committee Members,	Mary Bryk
	Robert Chapkin
Head of Department,	Gregory Reinhart

December 2017

Major Subject: Biochemistry

ABSTRACT

We have previously shown that partial inhibition of mitochondrial complex I activity with a small molecule tricycle pyrone compound (code name CP2) averted the development of cognitive and behavior phenotypes in multiple transgenic mouse models of Alzheimer's disease (AD). One of the beneficial effects of CP2 involved the protection against oxidative stress in primary mouse neurons, human cells and in mice fed with a high fat diet. In the current study, I investigated the molecular mechanism of CP2-induced neuroprotection and established the translational potential of this therapeutics using murine, human and Drosophila model systems. Target identification revealed that CP2 competes with a flavin mononucleotide (FMN) for the binding to the redox subunit of mitochondrial complex I. Bioenergetics studies showed that CP2 mildly inhibits basal cellular respiration simultaneously leading to a dose-dependent generation of a sub-lethal level of reactive oxygen species (ROS). This increase in ROS rapidly activates cytosolic signaling pathways including the nuclear factor erythroid 2-related factor 2/antioxidant response element (NRF2/ARE) activation to induce a protection against oxidative stress. This retrograde response is known as mitohormesis, and the genetic validation of this phenomenon was done in the longevity studies in several model organisms including Drosophila and C. elegans. Mitohormetic nature of CP2-induced protection against oxidative stress was confirmed using pharmacological and genetic manipulations in human cells, in Drosophila, and in the ARE reporter mice *in vivo*, and validated in mouse models of the AD. CP2 treatment also reduced the extent of

oxidative damage and enhanced the survival in wild-type (WT) mice fed with a high fat diet (HFD), which could be attributed to mitohormetic induction of the NRF2/ARE pathway. In summary, this study provides compelling evidence that mitohormetic activation of the NRF2/ARE pathway using small molecule partial inhibitor of mitochondrial complex I could be beneficial in multiple human conditions where oxidative stress contributes to the disease phenotype.

ACKNOWLEDGEMENTS

I would like to thank my research supervisor at the Mayo Clinic Dr. Eugenia Trushina for giving me the opportunity to pursue my Master's thesis in her lab. It enabled me to work on an intersection of mitochondria neurobiology and pharmacology, which resonated perfectly with my research interests and background. I would also like to thank the committee chair Dr. Paul Lindahl, and my committee members, Dr. Mary Bryk, Dr. Robert Chapkin for their guidance and support throughout the course of this master's program. Special thanks to the College of Agriculture and Life Sciences Prof. David Reed and Chair of Graduate Program of Biochemistry Dr. Mary Bryk at Texas A&M to allow me to work at the Mayo Clinic during my thesis. Thanks also go to Rafael Almanzar at Texas A&M for all his support and help. I would also like to thank my previous supervisor Dr. Fabiana Perocchi at Gene Center, Munich for introducing me to the wonderful field of mitochondria and giving me an opportunity to learn experimental biology and develop critical thinking, which helped me a lot during my graduate studies.

Many thanks also go to my colleagues at the Mayo Clinic (Dr. Sergey Trushin, Dr. Jordan Wilkins, Dr. Christopher Groen, Dr. Benjamin Gateno, Maxim Trushin, Dr. Andrea Stojakovic and Dr. Padraig Flannery) for helping me out with my experiments and making my time at the Mayo Clinic a great experience.

Finally, thanks to my family for their encouragement, patience, and support throughout my academic career.

CONTRIBUTORS AND FUNDING SOURCES

This work was supervised by a thesis dissertation committee consisting of Dr. Paul Lindahl, Department of Biochemistry at Texas A&M University as chair and Dr. Eugenia Trushina, Department of Neurobiology at Mayo Clinic along as research supervisor, with committee members as Dr. Mary Bryk, Department of Biochemistry at Texas A&M University and Dr. Robert Chapkin, Department of Microbial and Molecular Pathogenesis at Texas A&M University.

All work for the thesis was completed by the student and collaborators in the lab of Dr. Eugenia Trushina with the regular assessment from the Chair and thesis committee members. The thesis also includes the work of collaborators namely Dr. Alexander Galkin, Department of Neuroscience at Brain and Mind Institute, Weil Cornell Medical College; Prof. Michael K. Lee, Department of Neuroscience, University of Minnesota; Dr. Devin Oglesbee, Co-Director, Clinical Biochemical Genetics Laboratory, Mayo Clinic.; Dr. Eduardo N. Chini, Anesthesiology and Perioperative Medicine, Mayo Clinic.

Graduate study was supported by the Excellence fellowship from Texas A&M University for 1st year and the 2nd year was funded by the research grant provided by Dr. Eugenia Trushina. This project was supported by the Alzheimer Drug Discovery Foundation, NIH NIEHS R01 ES020715, Bright Focus Foundation A2011084, and the Mayo Clinic Stimulus Award Grant UL1 TR000135 from the NCATS (all to ET)

NOMENCLATURE

AD	Alzheimer’s disease
AMPK	AMP-activated protein kinase
AP1	Activator protein 1
APOE	Epsilon4 allele in apolipoprotein
APP	Amyloid Beta precursor protein
ARE	Anti-oxidant Response element
Aβ	Amyloid Beta
CALCOCO2	Adaptor protein calcium binding and coiled-coil domain 2
CHAPS	3-((3-cholamidopropyl) dimethylammonio)-1-propanesulfonate
Cncc	Cap'n'collar subfamily of leucine zipper
Cybrid	Cytoplasmic hybrid
DEA	Diethanolamine
E17	Embryonic day 17
ELOD	Early-onset AD
ETC	Electron Transport Chain
FACS	Fluorescence activated cell sorting
FAD	Familial AD
FMN	Flavin mononucleotide
GAPDH	Glyceraldehyde 3-phosphate dehydrogenase
GSK-3β	Glycogen synthase kinase 3β

GWASs	Genome-wide association studies
HFD	High-fat diet
HIF	Hypoxia induced factors
HMO1	Heme Oxygenase 1
HNE	4-hydroxynonenal
hPAP	Human placental alkaline phosphatase
IGF-1	Insulin growth factor-1
IL	Interleukin
iPSCs	Induced pluripotent stem cells
KEAP1	Kelch-like ECH-associated protein 1
LOAD	Late-onset AD
MAP2	Microtubule-associated proteins
MDA	Malondialdehyde
mt-DNA	Mitochondrial DNA
mTOR	Mammalian target of rapamycin signaling
MTT	3-(4,5-dimethylthiazol-2-yl)-2,5-diphenyl tetrazolium bromide
NF-κB	Nuclear factor kappa-light-chain-enhancer of activated B cells
NRF2	Nuclear factor erythroid 2–related factor
OXPHOS	Oxidative Phosphorylation
PEG	Polyethylene glycol
PSEN1	Presenilin 1
PSEN2	Presenilin 2

Rec-3	Renal epithelial cells
RLU	Relative luminescence units
ROS	Reactive Oxygen Species
RP-49	Ribosomal subunit-49
TBA	2-thiobarbituric acid
UPR	Unfolded protein response

TABLE OF CONTENTS

Page

LIST OF FIGURES

Page

1. INTRODUCTION

1.1. Etiology of Alzheimer’s disease

Alzheimer's disease (AD) is the most common type of cognitive dysfunction, accounting for about 60% of all dementias [1]. AD is a devastating, progressive, age-related brain disorder that affected ~ 44 million people worldwide in 2015 [2]. It leads to the loss of neurons in brain regions involved in learning and memory including the temporal and frontal lobes.

AD is clinically characterized by progressive memory decline and other cognitive deficits, including impaired judgment, decision-making and language disturbances. Definitive diagnosis of AD requires postmortem examination of the brain and is made on the presence of “plaques” and “tangles” [3]. Plaques are extracellular deposits of fibrils and amorphous aggregates that include amyloid beta peptides (Aβ). In a healthy brain, these protein fragments are broken down and eliminated. In Alzheimer's disease, the fragments accumulate to form hard, insoluble plaques. Neurofibrillary tangles are intracellular fibrillary aggregates of hyper-phosphorylated microtubule-associated protein tau [4]. Along with the molecular pathology, reduction in synaptic density and neuronal loss in some specific brain regions, including the cerebral cortex and hippocampus, are also important criteria for the diagnosis of AD [5].

The early-onset AD affects people ranging from 30-65 years of age and accounts for approximately 5% of total cases. It is associated with mutations in amyloid precursor protein (APP) [3], presenilin 1 (PSEN1) [4], and presenilin 2 (PSEN2), and is referred to as familial AD (FAD) [5]. However, most AD cases are sporadic with unknown genetic causes. Age is the greatest risk factor for the development of sporadic late-onset AD (LOAD). In recent years, extensive genetic evaluation identified risk factors for the development of LOAD where epsilon4 allele in Apolipoprotein (APOE4) gene is one of them [6]. Currently, AD has no cure. Lack of the detailed understanding of the disease mechanism hinders the development of efficacious therapeutic strategies. Therefore, the identification of early molecular mechanisms of AD and novel targets to halt the disease is of high priority.

1.2. Amyloid cascade hypothesis

Based on genetic etiology associated with the familial AD, the amyloid cascade hypothesis postulates that the neurodegeneration in AD is caused by abnormal accumulation of amyloid beta (Aβ) peptides in the brain [7]. Aβ is proposed to act as a pathological trigger for a cascade leading to the alterations in neuronal activity and synaptic loss caused by the formation of neurofibrillary tangles, which ultimately leads to neurodegeneration [7]. Aβ peptides, the major component of amyloid plaques, are 39–43 amino acid residue peptides proteolytically derived from the sequential enzymatic secretase on widely distributed transmembrane amyloid precursor protein (APP) [8, 9].

The length of Aβ peptide varies at C-terminal according to the cleavage pattern of APP. While cleavage of APP at the plasma membrane by the α-secretase occurs without formation of pathologic Aβ peptides, cleavage with β and γ-secretases leads to the release in the extracellular space of peptides with 40 or 42 residues which are prone to aggregation and represent the major component of extracellular amyloid plaques [10]. Further, the PS1 or PS2 mutations found in patients with FAD have specifically enhanced γ-secretase mediated cleavage to generate amyloidogenic Aβ42 peptides. However, the mechanism by which APP processing that leads to the formation of Aβ40 or Aβ42 is triggered in sporadic AD patients is still not well understood and probably represents one of the most important missing links in the understanding of this devastating disease. Despite the extensive evidence to support Aβ-driven neurodegeneration, all strategies designed to reduce the production of Aβ by blocking the activity of β or γ secretases, preventing Aβ aggregation, or promoting Aβ clearance by immunotherapy have failed clinical trials emphasizing the urgent need for the development of new therapies for AD [11].

1.3. Mitochondrial cascade hypothesis

Although the amyloid cascade hypothesis provides a plausible explanation of the underlying pathogenesis of the familial form of AD, it does not explain the late-onset, sporadic type of the disease, which accounts for 95% of AD cases [12]. First, individuals affected with the sporadic form of AD generally lack mutations in the genes associated with APP processing (APP/PS1/PS2). Second, plaques are a relatively common finding in the non-demented elderly [13]. Therefore it is currently unclear what factors are responsible for AD in these sporadic cases.

The mitochondrial cascade hypothesis asserts that mitochondrial function declining with age initiates pathological changes associated with AD and therefore represents the primary underlying problem in sporadic AD [12]. The initial validation of this hypothesis came from studying cybrid cell lines generated by fusing platelets from AD patients (donor cells) with neuroblastoma SH-SY5Y cells (rho 0 cell) that were depleted of mitochondrial DNA (mtDNA). This process creates cytoplasmic hybrid (cybrid) cells where the mtDNA from the donor is expressed in the nuclear and cellular background of the host rho 0 cells. Differences in phenotype between disease and control groups can thus be attributed to the exogenous mitochondria and mtDNA. Indeed, AD cybrid cell lines showed compromised electron transport chain activity, elevated levels of free radical production and oxidative stress markers, altered calcium homeostasis, activated stress signaling pathways, reduced mitochondrial membrane potential, and an increase in

the level of Aβ40 and Aβ42 production compared to the cybrid cell lines with mitochondria from control subject [14, 15]. Further, it has been specifically shown that mitochondrial ROS was sufficient to induce the formation of Aβ plaques through the increased activity of β secretase and this effect was abolished when cells were treated with anti-oxidants, suggesting mt-ROS could explain the formation of amyloid plaques in the sporadic AD. Moreover, increased levels of Aβ could independently accelerate mitochondrial dysfunction contributing to further increase in production of Aβ forming a vicious cycle leading to synaptic dysfunction and memory loss [16] (Figure 1.1).

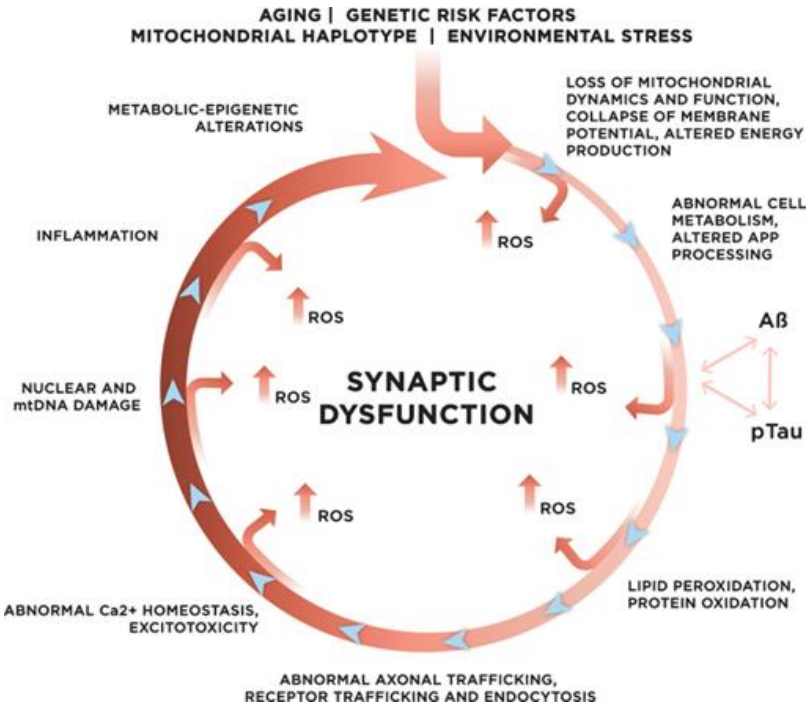

Figure 1.1. Abnormal mitochondrial dynamics and function could trigger the development of late-onset sporadic AD.
Reprinted from [17]

1.4. Oxidative stress is a major component of the underlying molecular mechanisms of AD

One of the major outcomes of mitochondrial dysfunction is oxidative stress caused by increased production of ROS [18]. Oxidative stress contributes to the development of numerous human neurodegenerative diseases [19]. Oxidative stress is the result of the unregulated production of reactive oxygen species (ROS) including hydrogen peroxide, nitric oxide, superoxide and hydroxyl radicals. The brain is particularly susceptible to the oxidative imbalance due to its high energy demand, high oxygen consumption, and rich abundance of easily peroxidizable lipids [20]. About 90% of cellular ROS is produced during mitochondrial respiration via OXPHOS and the activity of the electron transport chain (ETC) located in the mitochondrial inner membrane where energy is generated in the form of ATP [21]. OXPHOS consists of five multi-heterogenic complexes. During respiration, electrons are transferred from NADH and $FADH_2$ in the ETC via four membrane-bound complexes (complex I–IV) to oxygen, which finally generates water. As electrons are transported through complexes I, III, and IV, protons are pumped into the inner membrane space, generating an electrochemical gradient. This store of energy is used to generate ATP via the ATP synthase (complex V) (Figure 1.2). In this process, some electrons are leaking from the inner membrane and react with oxygen to form superoxide anions ($O^{2\cdot-}$). This can further react to generate other forms of ROS such as hydrogen peroxide (H_2O_2), hydroxyl radicals ($OH\cdot$), and hydroxyl ions

(OH^-). Reactive nitrogen species (RNS) are generated when $O2^{\cdot-}$ reacts with nitric oxide (NO) to form peroxynitrite ($ONOO^-$) [22].

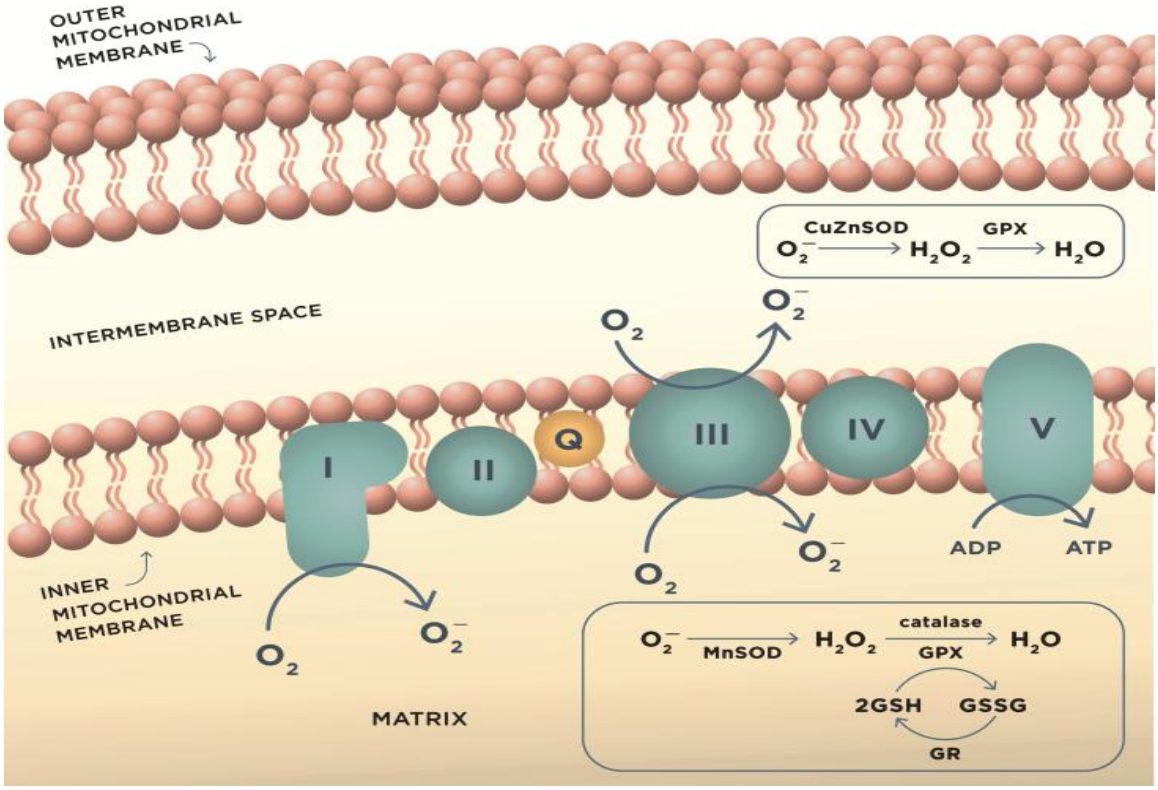

Figure 1.2. Oxidative phosphorylation machinery: Pathway for ATP generation and sites of ROS production in mitochondria.
Reprinted from [17]

Markers of oxidative stress including high levels of oxidized proteins, glycosylated products, extensive lipid peroxidation, formation of alcohols, aldehydes, free carbonyls, ketones, cholestenone, and oxidative modifications in RNA and nuclear and mitochondrial DNA were found in postmortem brain tissue and in peripheral cells and isolated mitochondria from people with preclinical or early stages of AD and ApoE4

carriers [17]. More recent studies showed significantly reduced activity of the antioxidant enzymes such as superoxide dismutase, glutathione peroxidase, and glutathione reductase in AD patients [23]. In another study, oxidative damage was reported to be the earliest event in AD followed by Aβ deposition [24]. Prevalence of oxidative damage in AD patients links the molecular chain of events initiated by mitochondrial dysfunction to AD pathology (Figures 1.1 and 1.2). Thus, it is feasible that inducing a protection against oxidative stress by activating intrinsic stress-response mechanisms that replenish the antioxidant cellular machinery could halt or reverse vicious cycle caused by mitochondrial dysfunction and delay the onset and/or slow the progression of AD (Figure 1.1).

1.5. Mitochondrial complex I as a therapeutic target

Cumulative evidence reveals that the regulation of mitochondrial turnover and function becomes impaired with ageing [25, 26]. Mitochondrial abnormalities include dysfunctional mitochondrial ETC activity, increased formation of ROS, shifted metabolic substrate utilization, aberrant mitochondrial dynamics (fission, fusion, axonal transport), and altered ion homeostasis [27]. Restoration of mitochondrial dynamics and function is currently considered as a therapy against many diseases [28]. However, strategies aimed to enhance mitochondrial activity via supplementation with the respiratory substrates or application of antioxidants failed in the clinical trials [29]. Unexpectedly, recent studies have shown that specific knock down of some genes

encoding for the subunits of complex I induce life-extension in worms and flies [30-33]. The increase in the lifespan has been attributed to mitohormetic ROS signaling that activates stress response. Moreover, analysis of the transcriptome of the long-lived species of N. Furzeri fish found a negative correlation between mitochondrial complex I activity and lifespan where pharmacological inhibition of complex I using a low dose of rotenone prolonged lifespan [34, 35]. An independent study using proteomics analysis demonstrated that low abundance of matrix arm subunits of complex I prolong life span in long-lived mice [36]. These studies further strengthen the fact that contrary to the increase in activity, partial inhibition of complex I through genetic or pharmacological means offsets ageing and could represent a drug target for age-related disorders. Furthermore, application of metformin, an FDA approved drug to treat diabetes, is also a partial mitochondrial complex I inhibitor, supports the safety of such approach in humans [37]. However, metformin does not penetrate the blood brain-barrier, and its application in AD models is controversial.

1.6. Mitohormesis: a mechanism triggered by complex I inhibition

To date, multiple studies have provided compelling evidence that partial inhibition of mitochondrial complex I increase longevity in model organisms including Drosophila, mice, C. elegans and N. Furzeri [38]. Investigations into the molecular mechanism behind this phenomenon revealed the presence of mitochondria-nuclear signaling where perturbations in mitochondrial function could be sensed by the nucleus leading to

changes in gene expression and chromatin remodeling [39]. This mito-nuclear communication helps the cell to maintain homeostasis under basal conditions and enables the adaptation to various stressors (Figure 1.3). Under mild stress conditions, mitochondria send "signals of distress" inducing a nuclear response that reconfigures cellular metabolism allowing the production of essential energy substrates and stress enzymes that provide both short-term cellular benefits and potential long-term adaptation [40, 41]. This phenomenon of non-lethal mitochondrial inhibition that stimulates stress response mechanism is known as mitohormesis. For example, beneficial effects of calorie restriction and exercise were explained by mitohormetic positive adaptation to stress induced by the transient generation of ROS in mitochondria [42]. ROS has been defined as the major signaling molecule of the mitohormesis, which is generated during inhibition of electron transport chain. While high levels of ROS are generally accepted to cause cellular damage and to promote ageing, low, sub-lethal levels of ROS serve as signaling molecules essential for many normal cellular functions [43]. The final validation of the beneficial effect of ROS came from studying the lifespan of C. elegans and Drosophila where the life-extending effects induced by calorie restriction or RNAi-mediated knockdown of mitochondrial complex I subunits were blocked by antioxidants [44-46]. The downstream signaling cascade associated with transiently increased ROS levels includes activation of p38, mitogen-activated protein (MAP) kinase, the transcription factors such as hypoxia-induced factors (HIF), antioxidant enzymes of unfolded protein response (UPR), innate immunity, autophagy, mitochondrial biogenesis, etc., which overall leads to better efficiency of cellular

functions, better clearance and turnover of aggregated proteins including Aβ and damaged mitochondria, and enhanced cellular energetics [40, 47, 48]. Together, these studies suggest that pharmacological agents that could trigger mitohormesis could provide alternative therapeutic strategies to promote healthy ageing and mimic the effect of caloric restriction and exercise.

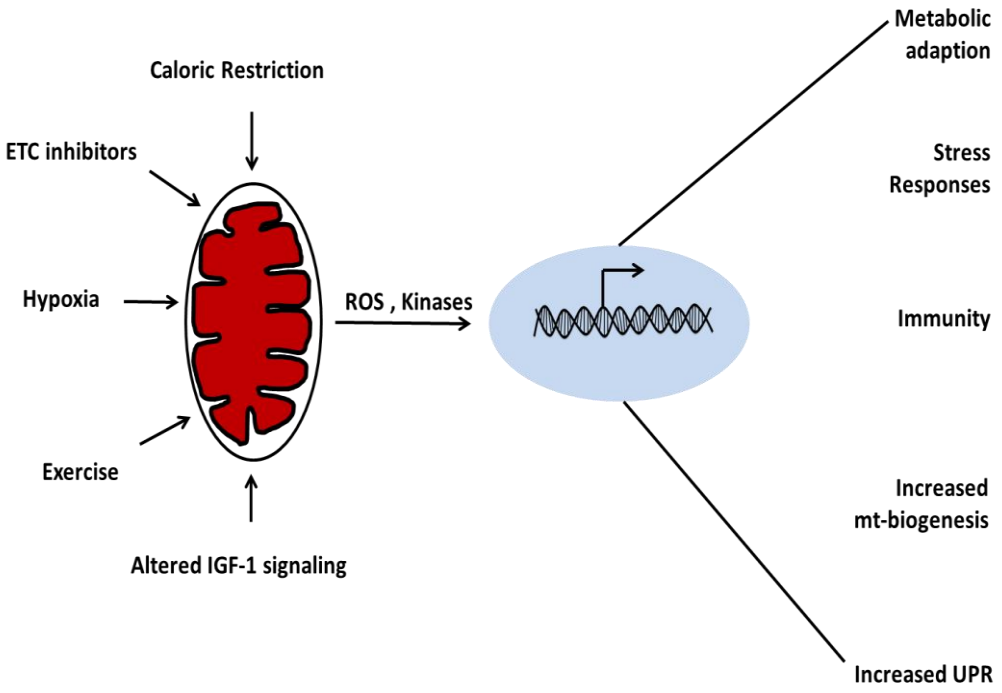

Figure 1.3. Multiple factors activate mitohormetic response.
Sub-lethal mitochondrial stress including ETC inhibitors, exercise, hypoxia, calorie restriction, and impaired glucose utilization through altered insulin growth factor-1 (IGF-1), activates signaling cascade leading to nuclear response known as mitohormesis. Mitohormesis provides adaptation to mild level of stress by increasing the production of respiratory substrates, activating autophagy and immunity, enhancing mitochondrial biogenesis and UPR activation.

1.7. Activation of the NRF2 pathway in neuroprotection

One of the most important outcomes of mitohormetic response is the activation of the transcription factor nuclear factor erythroid 2–related factor (NRF2) from the leucine zipper family [42]. NRF2 is a transcription factor and is the major regulator for the expression of over 200 genes that contain in their promoters the antioxidant response element (ARE) (Figure 1.4). These genes participate in phase I, II and III detoxification reactions, glutathione and peroxiredoxin/thyoredoxin metabolism, NADPH production, fatty acid oxidation, iron metabolism, proteasomal and autophagic processes, and gene regulation of other transcription factors [49]. NRF2 is tightly controlled at the level of protein stability by the ubiquitin E3 ligase adapter Kelch-like ECH-associated protein 1 (KEAP1). KEAP1 is a homodimeric E3 ligase adapter that contains several electrophilic and redox-sensitive cysteine residues. Under basal redox conditions, KEAP1 binds one molecule of NRF2 at two amino acid sequences with low (aspartate, leucine, glycine; DLG) and high (glutamate, threonine, glycine, glutamate; ETGE) affinity, respectively, and presents NRF2 to a complex formed by Cullin3/Rbx proteins leading to its ubiquitination and subsequent proteasomal degradation [50].

However, ROS and electrophiles are able to modify sulfhydryl groups of specific redox-sensitive cysteines of KEAP1, including C151, C273, and C288 [51]. Following these modifications, KEAP1 is no longer capable of presenting this protein for ubiquitination [52]. As a result, NRF2 escapes KEAP1-dependent degradation, accumulates in the

nucleus, and activates the expression of ARE genes. Several studies have suggested a KEAP1-independent mechanism for NRF2 activation that includes a direct phosphorylation of NRF2 mediating its translocation to the nucleus [53, 54].

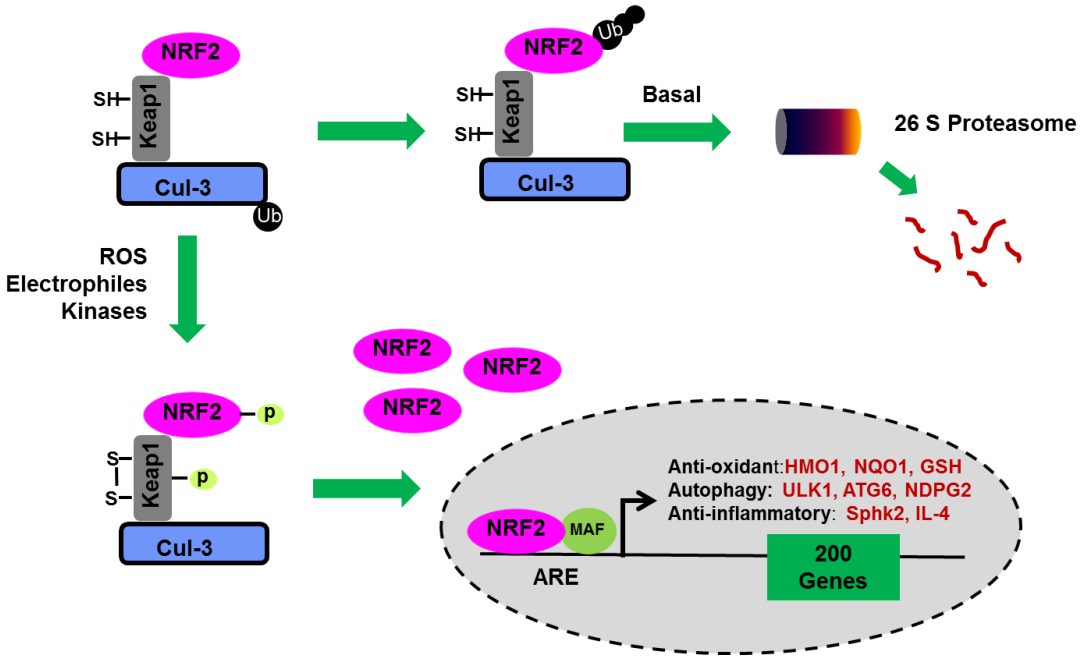

Figure 1.4. Mechanism of the NRF2 activation.
Under basal conditions, NRF2 is bound to KEAP1 and CUL3, which act as adaptors for ubiquitination followed by proteasomal degradation. In the presence of ROS, electrophiles or kinases, the cysteine residues of KEAP1 are modified that breaks the interaction between NRF2 and KEAP1 thereby facilitating NRF2 translocation to the nucleus initiating a transcription of the ARE genes.

Several important findings connect NRF2 to AD mechanisms. In hippocampal neurons of AD patients, NRF2 is predominantly cytoplasmic, suggesting the impaired capacity of these neurons to reduce proteotoxic and oxidative stress through NRF2-dependent transcription of cyto-protective genes. NRF2 overexpression *in vitro* protects against neurotoxicity of Aβ peptides and is associated with increased expression of NRF2 target genes and reduced oxidative stress [55]. Lentiviral overexpression of NRF2 in the hippocampus of old mice expressing mutant APP and PS1 transgenes was able to prevent spatial learning deficits [55]. Moreover, studies in NRF2-/- mice have shown the presence of amyloidopathy or tauopathy hallmarks [56, 57]. Hence, even in the absence of human transgenes involved in FAD, lack of the NRF2 expression in NRF2-/- mice resulted in the development of cognitive deficit that correlated with spontaneous tau aggregation [58]. Activation of the NRF2 pathway reduced levels of phosphorylated tau via induction of an autophagy adaptor protein calcium binding and coiled-coil domain 2 (CALCOCO2) in neurons [58]. Recently, a new mechanism of direct inhibition of inflammation by NRF2 has been reported, in which NRF2 activation suppresses macrophage and microglia inflammatory response by blocking the expression of pro-inflammatory cytokine genes such as Interleukin-6 (IL-6) and repressing transcriptional activity of nuclear factor kappa-light-chain-enhancer of activated B cells (NF-κB) [59, 60]. Altogether, this data strongly suggest that NRF2 deficiency exacerbates oxidative stress, neuro-inflammation and protein aggregation, the major pathways involved in AD pathophysiology (Figure 1.1). Moreover, antioxidant therapy based on the up-regulation of NRF2 has several important advantages over antioxidant supplementation since NRF2

activation will enhance the endogenous antioxidant metabolism (NADPH, Glutathione, and thioredoxin) in local places where needed while leaving physiological ROS signaling intact.

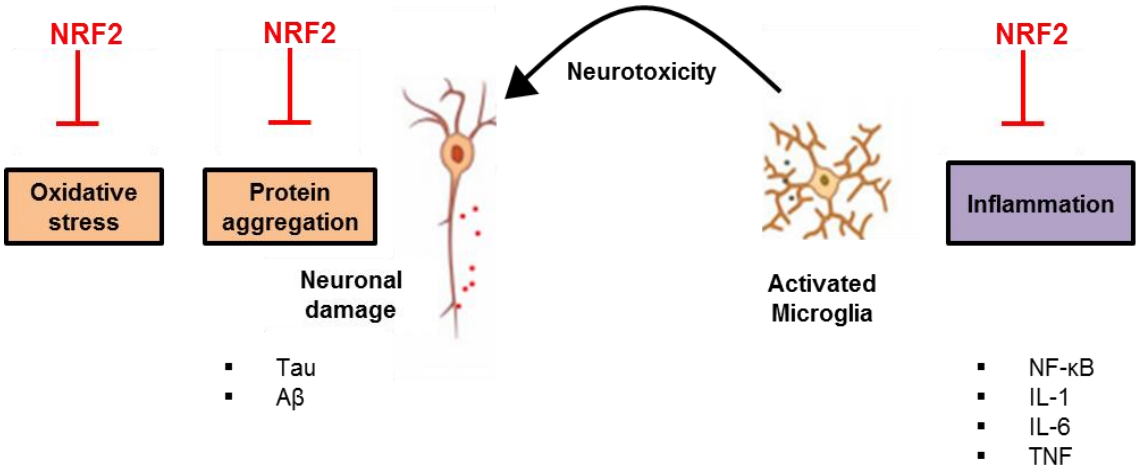

Figure 1.5. NRF2 provides neuroprotection via multiple pathways.
NRF2 initiates the transcription of genes that mediate oxidative stress response, proteasomal degradation of proteins and autophagy process thereby reducing Aβ and Tau aggregates. NRF2 also suppresses the production of pro-inflammatory cytokines from microglia and macrophages reducing inflammation and neurotoxicity.

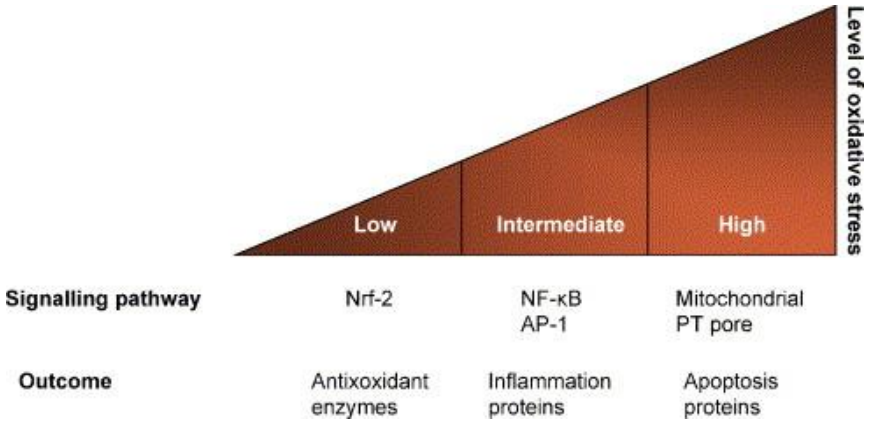

Figure 1.6. Hierarchical oxidative stress model.
A low oxidative stress induces NRF2, a transcription factor implicated in the activation of the expression of genes coding for antioxidant enzymes. An intermediate amount of ROS triggers an inflammatory response through the activation of NF-κB and AP1, and a high amount of oxidative stress induces apoptosis.
Reprinted from [61].

It is important to note that depending on the level of ROS, different redox-sensitive transcription factors are activated and coordinate distinct biological responses as shown in Figure 1.6. A low oxidative stress induces activation of a transcription factor NRF2 implicated in the activation of genes coding for antioxidant enzymes. An intermediate amount of ROS triggers an inflammatory response through the activation of NF-κB (nuclear factor kappa-light-chain-enhancer of activated B cells) and AP1 (Activator protein 1), and a high level of oxidative stress induces perturbation of the mitochondrial permeability transition pore and disruption of the electron transfer, thereby resulting in apoptosis or necrosis. Since mitohormesis is mediated by low level of ROS, hence it should only involve the activation of NRF2 signaling pathway, not the other transcriptional factors that are activated at high ROS level like NF-κB and/or AP1 and must not induce any toxicity

1.8. Small molecule complex I inhibitor CP2 induces neuroprotection in AD

Failure of recent clinical trials that targeted Aβ production and clearance indicates that amyloidopathy alone provides an incomplete view of disease urging the need for a discovery of new drug targets for AD. In the previous study, we demonstrated that partial inhibition of mitochondrial complex I with a small molecule CP2 induced neuroprotection preserving cognitive function in multiple mouse models of familial AD when independent cohorts of APP, PS1, and APP/PS1 mice were treated *in utero*, at pre- or symptomatic stages of the disease [62]. Partial inhibition of complex I is known to prolong the lifespan in multiple model organisms [35, 36]. However, our study was the first to show that this approach could be beneficial in AD. Extensive mechanistic and target identification studies revealed that CP2 penetrates the blood brain barrier, and accumulates in mitochondria where it competes with the flavin mononucleotide (FMN) for binding to the redox center of complex I [62, 63]. Molecular mechanisms induced by partial inhibition of complex I activity using CP2 included activation of AMP-activated protein kinase (AMPK); increased mitochondrial biogenesis and enhanced cellular energetics; increased autophagy and a reduction of soluble and insoluble levels of Aβ and pTau; inhibition of the activity of glycogen synthase kinase 3β (GSK-3β), restoration of axonal trafficking, increased levels of brain-derived neurotrophic factor (BDNF) and synaptic proteins. Interestingly, it was also found that CP2 induces a protection against oxidative stress in primary mouse neurons (Figure 1.7 A). In order to demonstrate a translational potential of this mechanism, experiments with human

neuronal cells derived from induced pluripotent stem cells were conducted in the laboratory of Dr. Carman at InVitro Cell Research, LLC, Englewood, NJ. It was found that CP2 also protected against oxidative stress in human neuronal cells. (Figure 1.7 B).

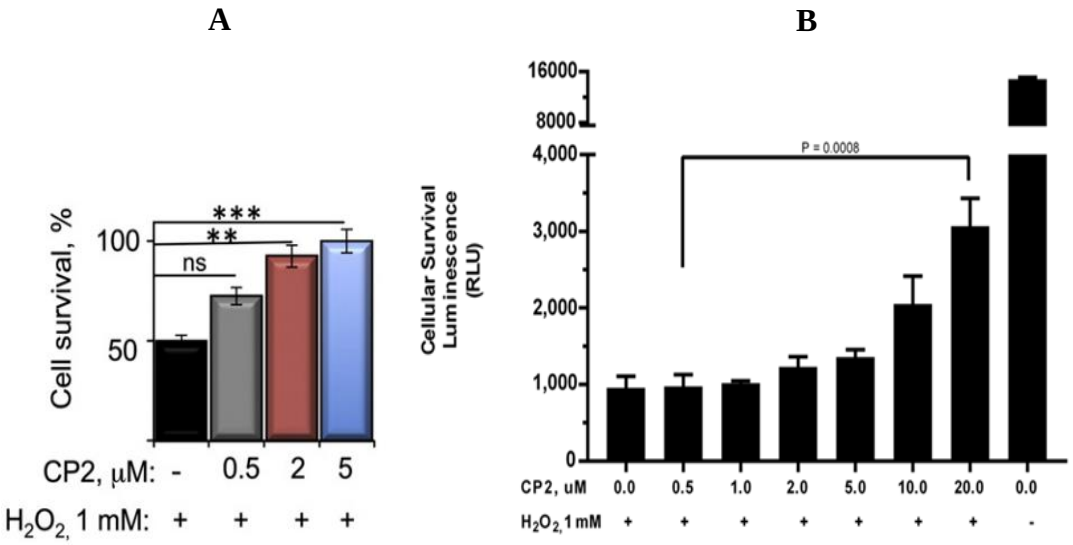

Figure 1.7. CP2 protects against oxidative stress in primary mouse neurons (A) and in human neuronal cells (B).
Cells were treated with 0.5 – 5 μM CP2 (A) or 0.5 – 20 μM of CP2 (B) for 24 hours, followed by treatment with 1 mM H_2O_2 for 2 hours followed with the measurement of cell survival. Figure (A) Reprinted from [62].
Figure (B) obtained from the unpublished results of Dr. Carman laboratory, InVitro Cell Research.

Furthermore, in order to validate that CP2 could protect against oxidative stress *in vivo* Trushina's lab examined a survival of WT mice fed with a high fat diet (HFD). HFD treatment represents an established *in vivo* model of oxidative stress where animals develop multiple tumors and die prematurely. Two groups of one-year old WT female

mice, ten animals in each group, were treated either with a HFD or with a HFD + CP2 (25 mg/kg/day via drinking water *ad lib*) till 2.5 years of age. It was found that CP2 treated mice fed with a high fat diet demonstrated enhanced health and life span (Figure 1.8). All animals in a HFD group developed multiple tumors confirmed during the postmortem tissue examination while none of the animals in HFD+CP2 group developed tumors.

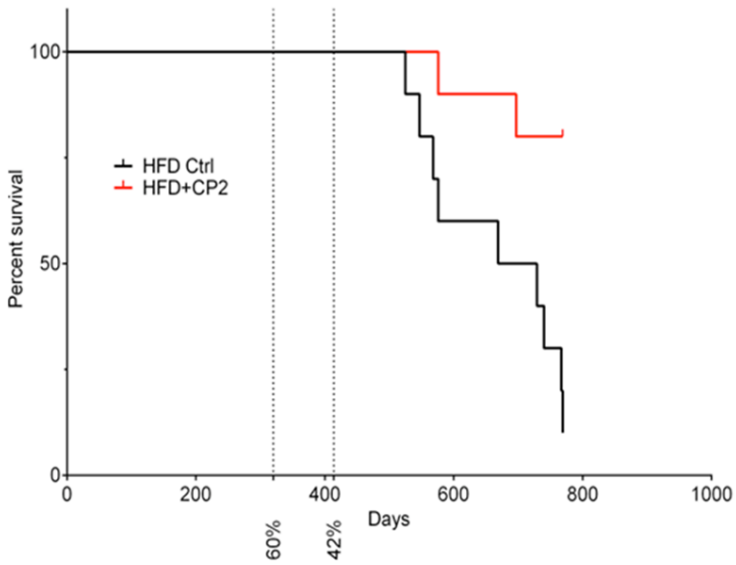

Figure 1.8. CP2 promotes a survival in WT mice fed with a HFD.
CP2 treatment (25mg/kg/day via drinking water ad lib) induces a protection against oxidative stress in WT mice fed a HFD. Survival of mice on CP2 was compared to vehicle-treated mice (n=10 in each group).
Figure obtained from the unpublished results of Dr. Trushina's and Dr. Chini laboratory, Mayo Clinic.

Since CP2 partially reduces complex I activity and mitochondrial respiration, it was examined whether CP2 leads to a generation of ROS in mitochondria isolated from

mouse brain tissue. These experiments were conducted in collaboration Dr. Galkin, Weil Cornell, NY. At CP2 concentrations previously shown efficacious for protection against oxidative stress *in vivo* and *in vitro* (> 20 µM), it was confirmed that CP2 partially inhibited mitochondrial respiration in agreement with our previous studies [67]. It was also found that at these concentrations CP2 produced a low level of ROS (Figure 1.9), which could act as signaling molecules for various transcriptional factors.

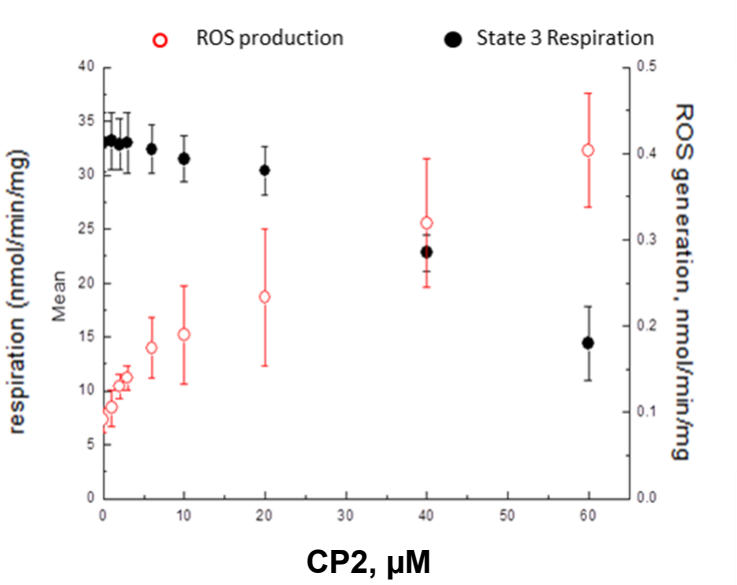

Figure 1.9. CP2 induces a dose-dependent inhibition of respiration and an increase in ROS levels in mitochondria isolated from the mouse brain tissue.
Mitochondria isolated from the mouse brain tissue were used for measurement of ROS production and respiration after CP2 treatment (0 - 60 µM). Two individual mitochondrial preparations were used for experiments, and each data point represents a mean of three independent measurements.
Figure obtained from the unpublished results of Dr. Galkin laboratory, Weil Cornell.

My project was focused on dissecting the molecular mechanism of CP2-induced protection against oxidative stress using multiple model systems. Detailed investigation

of the molecular mechanism involved in this phenomenon could advance the understanding of the fundamental mechanisms of stress resilience induced by mitochondria and aid the development of novel therapeutic strategies applicable to multiple human conditions.

2. RESEARCH AIMS

The overall goal of this study was to determine the molecular mechanism involved in a protection against oxidative stress induced by partial inhibition of mitochondrial complex I with a small molecule CP2.

2.1 Specific Research Aims

Aim 1. Investigate the molecular mechanism of CP2-induced protection against oxidative stress

1.1. Examine whether CP2 is an antioxidant.

1.2. Examine whether partial inhibition of mitochondrial complex I using CP2 induces the NRF2 activation via mitohormesis *in vitro* and *in vivo*.

Aim 2. Using genetic manipulations in Drosophila, confirm that NRF2 activation is essential for a CP2-induced protection against oxidative stress.

Aim 3. Validate that enhanced survival found in CP2-treated wild-type mice fed with a high fat diet was linked to the reduction of oxidative damage.

3. MATERIAL AND METHODS

3.1. Cells

ARE HEPG2, AP1 HEK293, and NF-κB HEK293 reporter cells were purchased from BPS biosciences (Catalog# 60513, 60405, and 60650 respectively).

3.2. Animals

Animal care and handling procedures were approved by the Mayo Clinical Institutional Animal Care and Use Committee in accordance with the National Institutes of Health's Guide for the Care and Use of Laboratory Animals. Drosophila strains were purchased from Bloomington Drosophila Stock Center at Indiana University include female elavGal4 (8760) and male attp2 (36303), NRF2 RNAi (25984). All flies were kept at 25°C. Control or NRF2 RNAi Drosophila lines were created by crossing elavGAL4 virgin females with attp2 or NRF2 RNAi males. For studies with mice fed a high- fat diet, C57Bl6 retired female breeders were purchased from Jackson's laboratory. CP2 treated ARE reporter mice brain tissue samples were provided by Dr. Michael Lee, University of Minnesota.

3.3. Reagents

CP2 was synthesized by Nanosyn, Inc using method described by Hua et al. (2003) and purified using HPLC. Neurobasal medium (Gibco, catalog# 21103-049), B27 supplement (Gibco, catalog# 17504-044), Glutamine (Gibco, catalog# 25030-032), penicillin-streptomycin (Penstrep, sigma, catalog# PO781), Poly-L-ornithine (Sigma, catalog# P3655), DMEM high glucose, 25 mM HEPES, no glutamine (Lonza, catalog# 12-709B), F-12 (Gibco, catalog# 11765-054), Serum, iron supplemented bovine calf serum (HYC, catalog# 2049), papain (Worthington, catalog# LK003176), mitosox (Thermo scientific, catalog# M36008)

3.4. CP2 preparation and treatment

For *in vitro* studies, CP2 was dissolved in polyethylene glycol (PEG) or 100% DMSO at final concentration of 50 mM. For experiments involved in treatment of the ARE reporter mice, CP2 was gavaged at a concentration of 25 mg/kg/day. For experiments with Drosophila, CP2 was mixed with 20% sucrose diet at concentration of 25 mg/kg/day.

3.5. Primers

The following primers were used for the quantification of the NRF2 homolog, cap'n'collar subfamily of leucine zipper (Cncc) expression levels in Drosophila. Primers were designed using NCBI primer designing tool. They were dissolved in dd H_2O_2 to obtain 10 µM final concentrations.

Forward primer Cncc: GTTTTCAAGCTCACCACCAAT

Reverse Primer Cncc: AAATTCGCAGTTTCCACGGC

3.6. Cell culture

HEPG2 ARE reporter cells and were cultured in the rich MEM low glucose complete media (Corning, catalog# 10-010CV) supplemented with 10% FBS (sigma, catalog# 2442), sodium pyruvate (Corning, catalog# MT25000CI), MEM non-essential amino acids (Corning, catalog# 25-025-CI).

3.7. Luciferase assay

HEPG2 ARE reporter cells were seeded in 96 well plates at a density of 30,000 cells per well and cultured for 24 hours. Cells were treated with 2.5 to 20 µM CP2 dissolved in PEG, followed by 24 hours incubation. Cells were washed with PBS and lysed in 30 µl of lysis buffer (50 mM Tris, 2.5 mM EDTA, 150 mM NaCl, 1% Triton and 0.25% of

NP-40). Luciferase activity was measured using Promega kit (Catalog# E1960). 100 µl of the substrate was added to 25 µl of lysate and luminescence was measured in luminometer with 500 ms integration time. Protein quantification was done to normalize the luminescence using BCA protein quantification kit (Bio-Rad, catalog# 500012) by measuring the absorbance at 750 nM.

3.8. Measurement of ROS levels in HEPG2 ARE reporter cells

ROS generation was measured in HEPG2 ARE reporter cells using mitosox (Thermo-scientific, catalog# M36008), which is a red mitochondrial superoxide fluorescent indicator. HEPG2 ARE reporter cells were seeded at a density of 0.5 million cells per well in 6 well plate and cultured overnight. There are two assays to measure ROS. First experiment demonstrate whether CP2 leads to ROS generation in HEPG2 ARE reporter cells, in which cells were treated with 5 µM mitosox in HBSS buffer for 10 min at 37°C, followed by 20 µM CP2 treatment for 1.5 hours. In the other experiment to determine at which time point of CP2 incubation, ROS production occurs, cells were treated with 20 µM CP2 or 50 µM antimycin for 5 min, 15 min, 45 min and 1 hour, media was removed and 5 µM mitosox in HBSS buffer was added for 10 min incubation at 37°C. In both the experiments, cells were trypsinised, collected in PBS + 5% FBS, and analyzed by flow cytometry at 488 nM excitation/580 nM emission wavelength. Results were analyzed using Cell quest software (BD Biosciences)

3.9. Cell viability assays

Cells were treated with 3-(4, 5-dimethylthiazol-2-yl)-2, 5-diphenyl tetrazolium bromide (MTT) reagent at 0.25 mg/ml followed by 4 hours of incubation at 37°C. Solubilization of MTT formazan was done by the addition of 200 µl of 40 nM HCl in isopropanol (2:1) to 100 µl of media for 10 min placed on a shaker, and absorbance was measured at 570 nM.

3.10. Quantitative PCR

To test for the m-RNA expression of NRF2 in the WT and NRF2 RNAi cross, one step q-PCR SYGR kit (Bio-Rad, catalog# 1725150) was used. Ribosomal subunit-49 (RP-49) was used as housekeeping gene for normalization. Samples were run in thermocycler in triplicates with following conditions: 10 min at 50°C (reverse transcription), 1 min at 95°C (polymerase activation), followed by 38 cycles of denaturing and annealing/ extension for 10 sec at 95°C and 30 sec at 60°C respectively. The data were analyzed by double delta Ct analysis.

3.11. Human placental alkaline phosphatase activity in ARE reporter mice

ARE activation after CP2 treatment was measured *in vivo* using ARE reporter mice by the quantification of human placental alkaline phosphatase (hPAP) enzyme activity in brain tissue collected after 4 days of CP2 treatment (gavage with CP2 25 mg/kg/day in PEG). Two to five mg frozen hippocampus brain tissue was homogenized in 1 mL TMNC buffer (50 mM Tris pH 7.5, 5 mM $MgCl_2$, 100 mM NaCl, and 4% 3-((3-cholamidopropyl) dimethylammonio)-1-propanesulfonate (CHAPS)). The homogenate was freeze-thawed, and 25 μL of lysate was added to a white-walled 96 well plate and mixed with 75 μL of 200 mM diethanolamine (DEA) buffers. Plates were incubated for 20 min at 65°C to inhibit endogenous phosphatases. Following the addition of 100 μL of substrate solution [2X CSPD (Applied Biosystems, catalog# T2041), 2X Emerald reagent (Applied Biosystems, catalog# T2115), 5 mM $MgCl_2$, and 150 mM DEA] and incubation in the dark for 20 min at room temperature, luminescence was measured using a microplate luminometer (Berthold Detection Systems, Pforzheim, Germany) with one second integration time. Luminescence values were normalized to protein concentration measured using bicinchoninic acid protein assay (Bio-Rad, catalog# 500012). ARE-hPAP activity was expressed as relative luminescence units (RLU) per mg of protein.

3.12. Estimation of lipid peroxidation

Lipid peroxidation was estimated by measuring the amount of malondialdehyde (MDA) using a calorimetric assay (Sigma, catalog# MAK085-1KT). 5 mg of the cortex and hippocampus tissues were isolated from WT mice fed with a high-fat diet from control (HFD alone), and CP2 treated mice (HFD+CP2) and were lysed in 300 µl of the MDA lysis buffer, centrifuged, and supernatant was transferred to another tube. 200 µl of sample or standard were aliquoted in different tubes, and 600 µl of 2-thiobarbituric acid (TBA) was added to each tube. The rest of the sample was diluted 5 times in lysis buffer for protein estimation (3 µl in 12 µl of lysis buffer). Samples were incubated for 1 hour at 95°C, centrifuged at 2000 g for 1 minute and the supernatant was separated. 200 µl of the adduct solution was added to each well of clear 96 well plate. Absorbance was read at 532 nM wavelength. Absorbance values were blank corrected and normalized for protein concentration.

3.13. Assessment of a total CP2 anti-oxidant capacity

To analyze the anti-oxidant capacity of CP2, I followed instructions provided in total antioxidant capacity assay kit (Sigma, catalog# MAK187). The quantification is based on the reaction where reduced Cu^{+} ion chelates with a colorimetric probe giving a broad absorbance peak at ~570 nm, which is proportional to the total antioxidant capacity. Various concentrations of a strong anti-oxidant trolox (4 - 20 µM/well) were used as

positive control. Further, 100 µL of Cu^{2+} working solution to both CP2 and trolox was added. Samples were incubated at room temperature for 90 min followed by absorbance measurement.

3.14 Neuronal culture from embryonic day 17 (E17) mice

Following reagents were prepared a day before neuronal culture in molecular grade water.

1. Hepes buffered Saline (HBS) (0% Ca^{2+} - 0% Mg^{2+}). For 500 ml:

    1.1. 4.2g NaCl
    1.2. 0.112g KCl
    1.3. 1.19g HEPES
    1.4. 0.5g glucose
    1.5. pH was adjusted to 7.3 with 1 N NaOH
    1.6. Solution was filtered sterile and stored at 4°C

2. Borate Buffer (500 ml):

    2.1. 2.38g boric acid
    2.2. 1.27g borax (sodium borate) in 400 ml H_2O
    2.3. pH was adjusted to 8.4 and volume to 500 ml
    2.4. Solution was filtered sterile and stored at 4°C

3. Poly-L-Ornithine: 0.5 mg/ml in borate buffer was prepared.

4. Papain solution: 2mg/ml in HBS was prepared.

5. Plating media :

    5.1. 400 ml DMEM
    5.2. 50 ml heat inactivated bovine calf serum. FBS was thawed at 56°C for 30 mins and swirled every 10 min, followed by 10 min incubation on ice and aliquoted to 50 ml tubes.
    5.3. 50 ml F-12

5.4. 1 ml Penstrep
5.5. Solutions were mixed and aliquoted into 50 ml conical tubes under sterile conditions and stored at 4°C.

6. Feeding media

6.1. 500 ml neurobasal media
6.2. 10 ml B27 supplement
6.3. 1 ml PenStrep
6.4. 125 µl of glutamine (200 mM) must be added prior to each feed to the individual 50 ml conical tubes
6.5. Solutions were mixed and aliquoted into 50 ml conical tubes under sterile conditions and stored at 4°C.

3.14.1. Procedure before dissection

1. Poly-L-Ornithine coating: 10 ml of 0.5 mg/ml of Poly-L-Ornithine in borate buffer was used to cover 10 cm dish and left overnight under the hood.
2. On the day of neuronal culture, Poly-L-Ornithine was aspirated with sterile pasteur pipette and washed 2x with sterile water.
3. Dishes were left under the hood to dry for 2-4 hours without lids.
4. Once dried, plate was covered with 10 ml of platting media and left in incubator until neurons were isolated for plating.

3.14.2. Preparation for dissection

1. All the dissecting instruments were sterilized in gauze at bottom, filled with Ethanol.
2. HBS was aliquoted into three 100 mm petri dishes and one 35 mm dish.
3. Plating medium was placed in 37°C water bath and 0.25 ml papain was aliquoted was placed inside hood in 15 ml tube.

3.14.3. Procedure to sacrifice the mouse

All procedures involving animals were approved by the Institutional Animal Care and Use Committee. All efforts were made to minimize animal suffering and to reduce the number of animals used.

1. Cervical dislocation method was used on the wild type murine pregnant mother at gestational day 17.
2. To sterilize and prevent hair contamination, mouse was placed on its back and ethanol was spared on the abdomen of the mouse until all hair gets wet.
3. Grabbing the abdominal muscle with the forceps a transversal incision was made. By inserting one of the blades of the scissors into the abdominal cavity a longitudinal incision was made to expose abdominal content.
4. Vagina was cut and uterus containing 17 days old embryo was removed and placed in 10 cm plate containing HBS buffer.

3.14.4. Extraction of brain tissue

1. With scissors, embryos were released from the placenta and then moved with the spoon to 10 cm petri dish with sterile HBS.
2. In the same dish, heads were cut and with the spoon, transferred into another 10 cm dish with HBS. This maintains cleaner conditions, which ensures maintaining sterile conditions for neuronal culturing.
3. To dissect the brain, tweezers were used to hold the head, and brain was exposed using the snip between the eyes and the back of the head to peel the top of the head.
4. Isolated brain was transferred to the second 10 cm petri dish with sterile HBS.

5. Forceps were used to split the hemispheres, and using olfactory blub as a landmark, meninges were removed. Further, hippocampus was also removed exposing the intact cortical tissue.
6. Cortex was clipped using forceps and collected into another 35 mm dish.

3.14.5. Neuronal cell plating

1. Once the cortex was collected from all hemispheres, tissue was transferred to the 15 ml conical tube containing papain solution using the sterile plastic pipette and incubated at 37°C for 20-30 min.
2. After papain digestion, cortex was transferred into 10 ml of plating media and homogenized using 1 ml pipette ~ 20 times.
3. Live neurons were counted using trypan blue on hemocytometer and cells were platted at a density of 35,000 cells per ml and kept in incubator at 37°C.
4. After 72 hours, media was changed to feeding media, which was supplemented with L-glutamine and cells were kept in incubator at 37°C for next 3 – 4 days.

4. RESULTS

4.1. CP2 does not possess anti-oxidant properties

In order to dissect the molecular mechanism of oxidative stress protection induced by CP2, I first determined whether CP2 has anti-oxidant properties. The total non-enzymatic anti-oxidant capacity of CP2 was accessed using a calorimetric assay kit (sigma, catalog# MAK187-1KT) that measures a reduction of the cupric ion to cuprous ion. I used this kit to determine whether 2.5 – 100 µM of CP2 could reduce Cu^{2+} to Cu^{+}. Cu^{+} chelates with a colorimetric probe and gives a broad absorbance peak at ~570 nm indicative of the total anti-oxidant capacity. Trolox, a known anti-oxidant, was used as a positive control. Trolox or CP2 were diluted to concentrations ranging from 0, 2.5, 10, 20, 50, and 100 µM in 100 µl of water in a clear 96 well plate. Two vehicle controls included PEG for CP2 and DMSO for trolox, respectively. 100 µl of solution containing Cu^{2+} working solution + probe was added to each well containing either CP2 or trolox samples and mixed by multiple pipetting. Plate was incubated in dark for 90 minutes at room temperature followed by absorbance measurement at 570 nM on a 96 well plate reader. Experiments were done in triplicates; data was plotted as mean +/- standard deviation. I found that CP2 does not behave as an anti-oxidant at concentrations ranging from 2.5 µM to 100 µM (Figure 4.1). I observed a small increase in absorbance at high concentrations of CP2 that, most likely, was due to its precipitation.

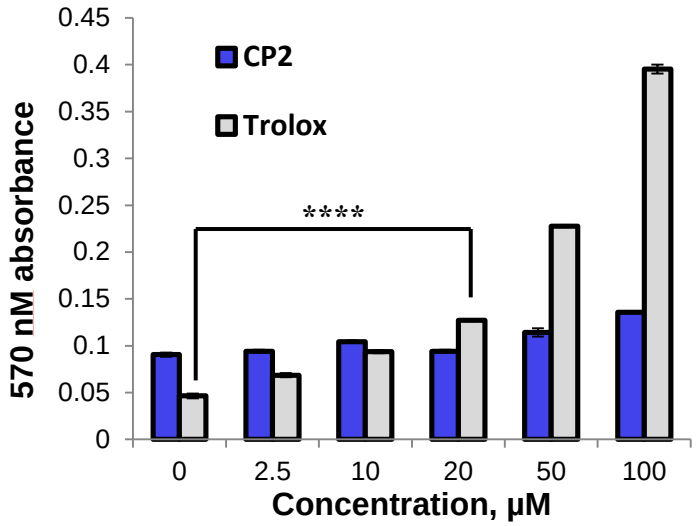

Figure 4.1. CP2 does not behave as an anti-oxidant.
Total non-enzymatic antioxidant capacity of CP2 compared to trolox was measured by quantifying the reduction of Cu^{2+} to Cu^{+}. Cu^{+} chelates with a colorimetric probe produces an absorbance peak at ~570 nm, which corresponds to a total antioxidant capacity. Graph is representative of two independent experiment and data is represented as mean +/- SD of triplicates; t-test was used for statistics, ****, $p < 0.001$.

4.2. CP2 specifically induces the NRF2 activation in HEPG2 reporter cells

Sub-lethal levels of ROS could facilitate mitochondria-nuclear communication via mitohormetic activation of protective mechanisms. From data generated with our collaborators, we learn that at concentrations of 0 - 20 µM, CP2 generates low dose of ROS in mitochondria isolated from mouse brain tissue. Depending on the levels, ROS are known to activate many transcriptional factors including NRF2, NF-κB and AP1. In order to confirm what pathways were activated after CP2 treatment, I tested the effect of CP2 on luciferase activity in NRF2 HEPG2 (BPS bioscience, catalog# 60513), AP1

HEK293 (BPS bioscience, catalog# 60405) and NF-κB HEK293 (BPS bioscience, catalog# 60650) reporter cell lines. These reporter cell lines stably expressed the luciferin gene tagged with an upstream binding sequence for NRF2, AP1 or NF-κB transcription factor. In order to perform these experiments, cell density for reporter cells was optimized for seeding in the 96 well plate, and 35,000 cells per well was found to be ideal. CP2 doze optimization was also done to determine its physiological concentrations in both HEPG2 and HEK293 reporter cell lines using the MTT assay. For MTT assay, 30,000 cells were seeded in 96 well plates following with the overnight incubation in rich MEM media. Next day, cell survival was measured using the MTT assay. It was found that CP2 did not induce any toxicity in HEPG2 reporter cells or HEK293 reporter cells at concentration up to 50 µM (Figure 4.2 A, B). Hence, I proceeded with using 0 - 20 µM of CP2 for the luciferase assay.

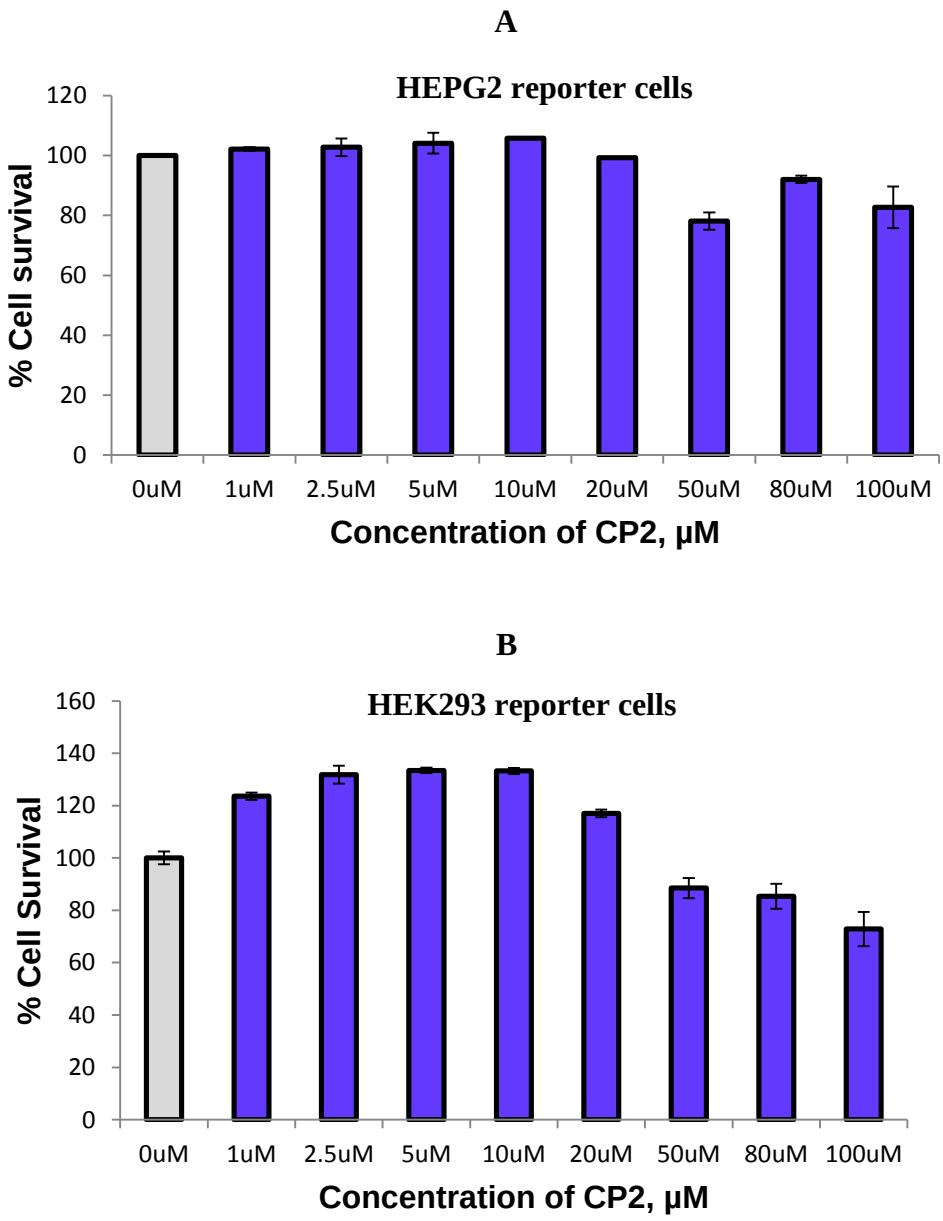

Figure 4.2. CP2 does not induce toxicity in HEPG2 (A) or HEK293 (B) reporter cells below 50 µM.

HEPG2 or HEK293 reporter cells were treated with 0 – 100 µM of CP2 for 24 hours followed by measurements of cell survival using the MTT assay. Both the graphs represent two independent experiments; data is presented as the mean +/- SE of five replicates.

For the measurement of luciferase activity, cells were incubated with different concentrations of CP2 (2.5 µM - 20 µM) dissolved in PEG; 10 µM sulforaphane used as a positive control (NRF2 activator); or 10 ng/ml of phorbol 12-myristate 13-acetate (PMA, a known NF-κB and AP1 activator); or PEG alone as a negative control for 8, 24 and 48 hours in 3 replicates. Cells were observed under the microscope for each well after respective incubation time, and no cell death was observed in cells treated with vehicle, CP2 or positive controls. Flow chart of experimental procedure is presented in Figure 4.3. After the incubation, cells were washed with PBS and lysed in 30 µl of lysis buffer. 25 µl of lysate was treated with luciferase chemiluminescent substrate, and luminescence was measured in a plate reader with 500 ms time of integration. Remaining 5 µl of the lysate was used for the protein quantification using the BCA assay (Bio-Rad # 500012), where standards were prepared in the same buffer as was used for cell lysis. Luminescence data was normalized by protein concentration for each well. I found that CP2 leads to the activation of NRF2 after 24 hours of incubation, which sustained till 48 hours (Figure 4.4). However, I also found that CP2 did not induce the activation of AP1 and NF-κB after 8, 24 or 48 hours (Figure 4.5 and 4.6). This signifies that CP2 leads to the generation of low ROS that is sufficient to activate NRF2 but not NF-κB and AP1 signaling pathways consistent with the mitohormetic mechanism. I observed that CP2 reduced AP1 and NF-κB activity, which could be due to the negative feedback signaling of NRF2 activation [61]. These results suggested that CP2 specifically activates NRF2 at concentration below the toxicity levels in reporter cells.

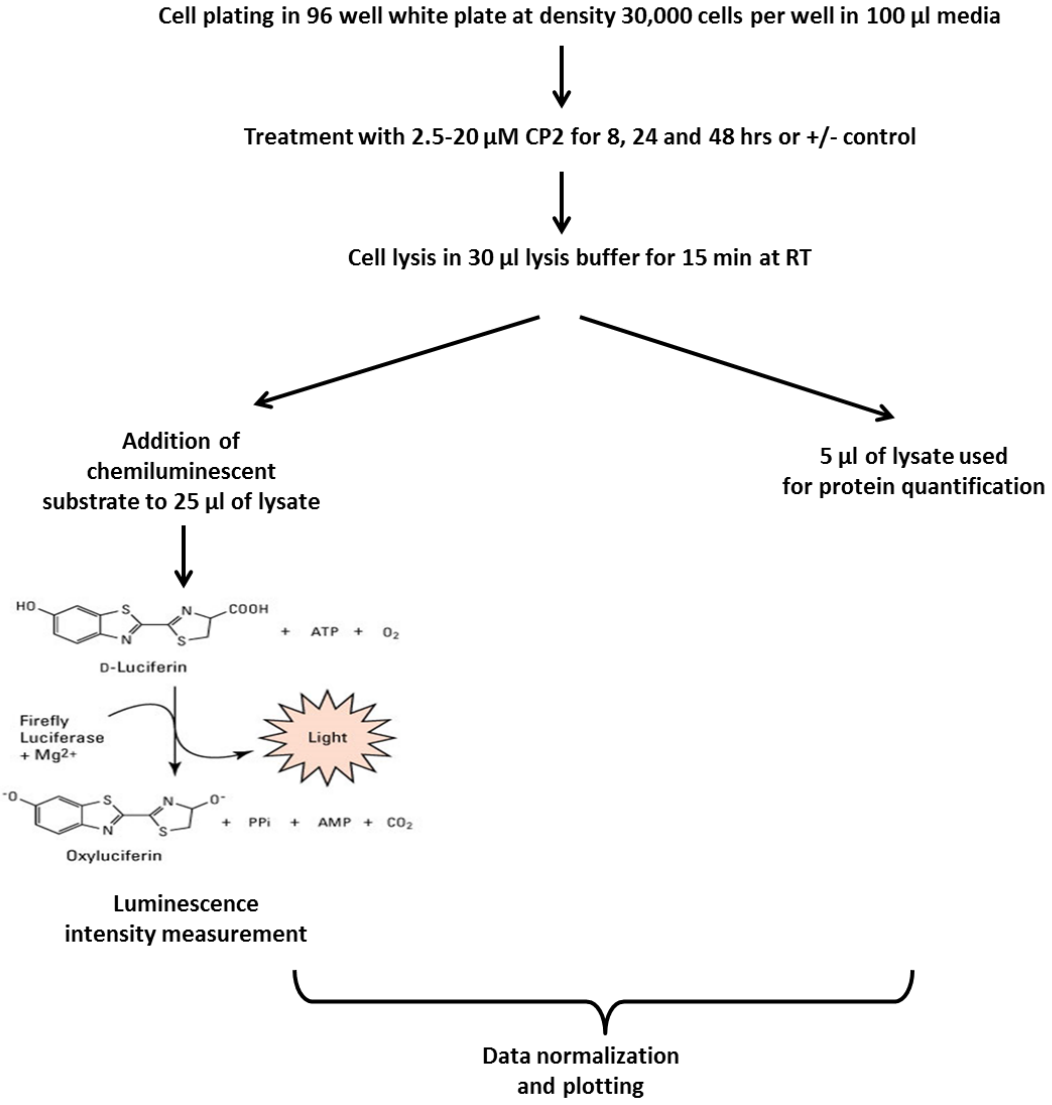

Figure 4.3. Experimental procedure to measure the luciferase activity in reporter cells.

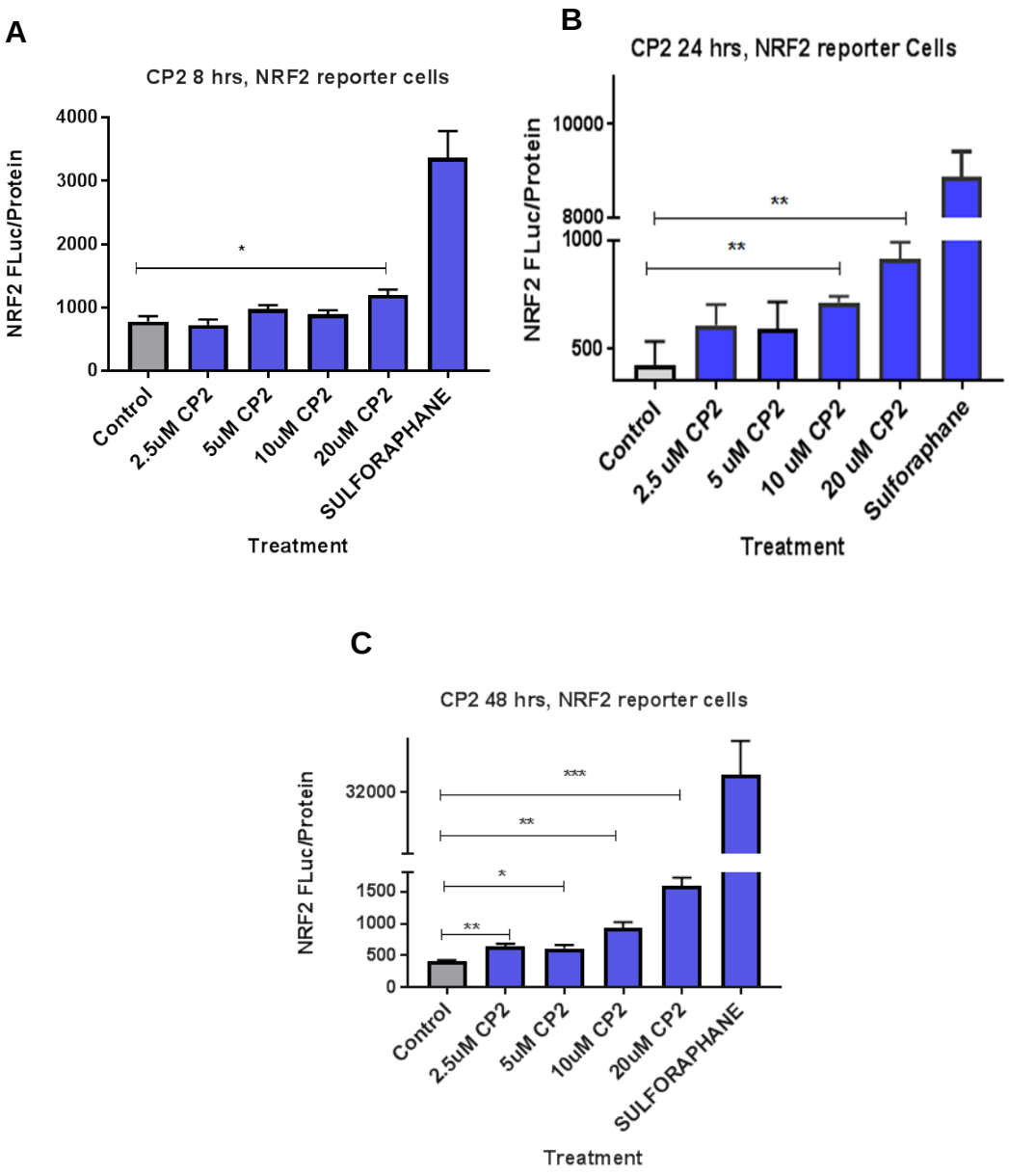

Figure 4.4. CP2 induces NRF2 activation in HEPG2 reporter cells.
NRF2 activation was measured after 2.5 µM- 20 µM CP2 treatment for 8 (A), 24 (B) and 48 (C) hrs using luciferase assay in HEPG2 reporter cells. Luminescence data was normalized to the protein concentration. All graphs represent data from three independent experiments. Data is presented as mean +/- SE of 3 replicates; t-test is used for the statistics, **, $p < 0.01$;***, $p < 0.005$

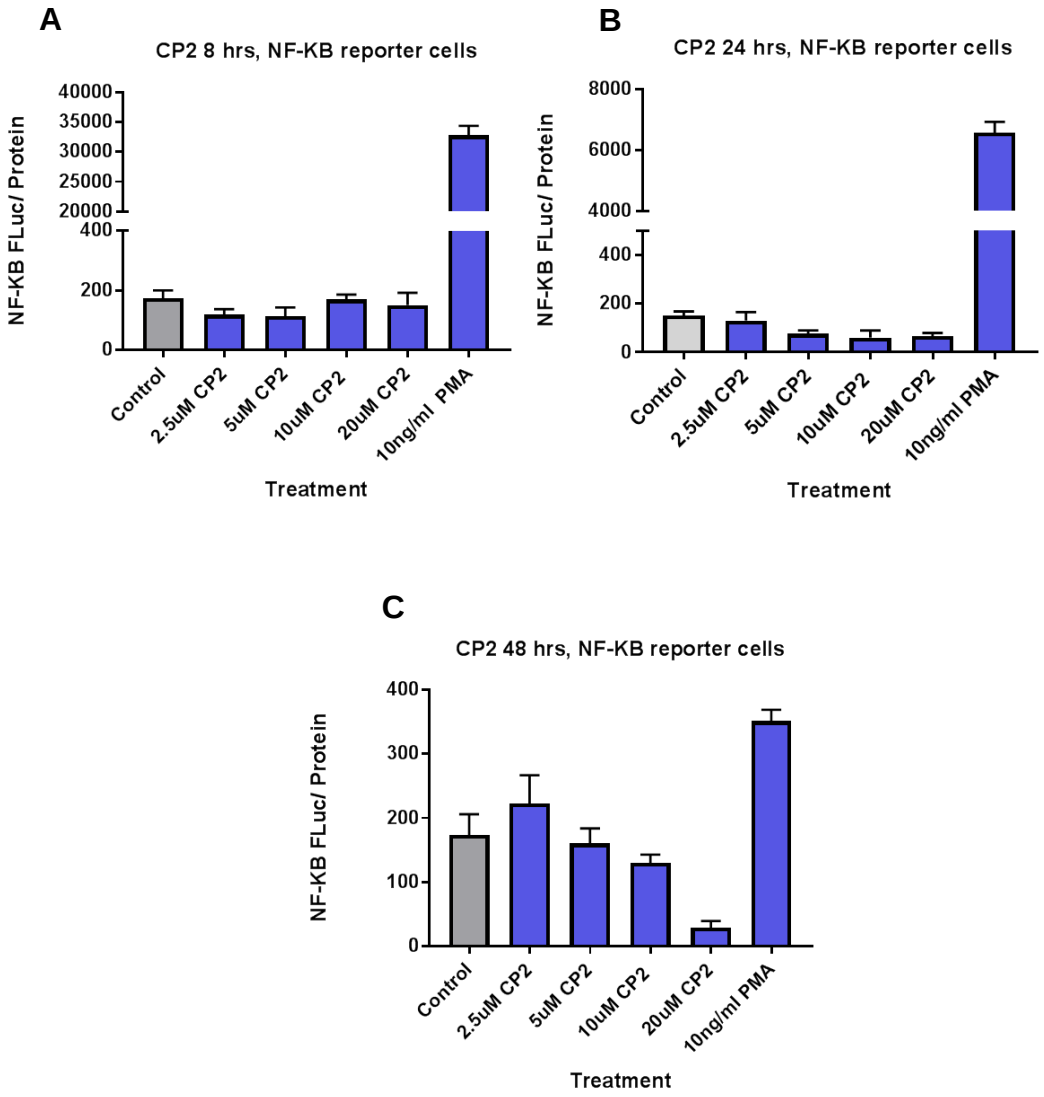

Figure 4.5. CP2 does not induce NF-κB activation in HEK293 reporter cells.
NF-κB activation was measured after 2.5 µM- 20 µM CP2 for 8 (A), 24 (B) and 48 (C) hrs treatment using luciferase assay in NF-κB HEK293 reporter cells. Luminescence data was normalized to the protein concentration. All graphs represent data from three independent experiments. Data is presented as mean +/- SE of triplicates; t-test is used for the statistics, **, $p < 0.01$;***, $p < 0.005$

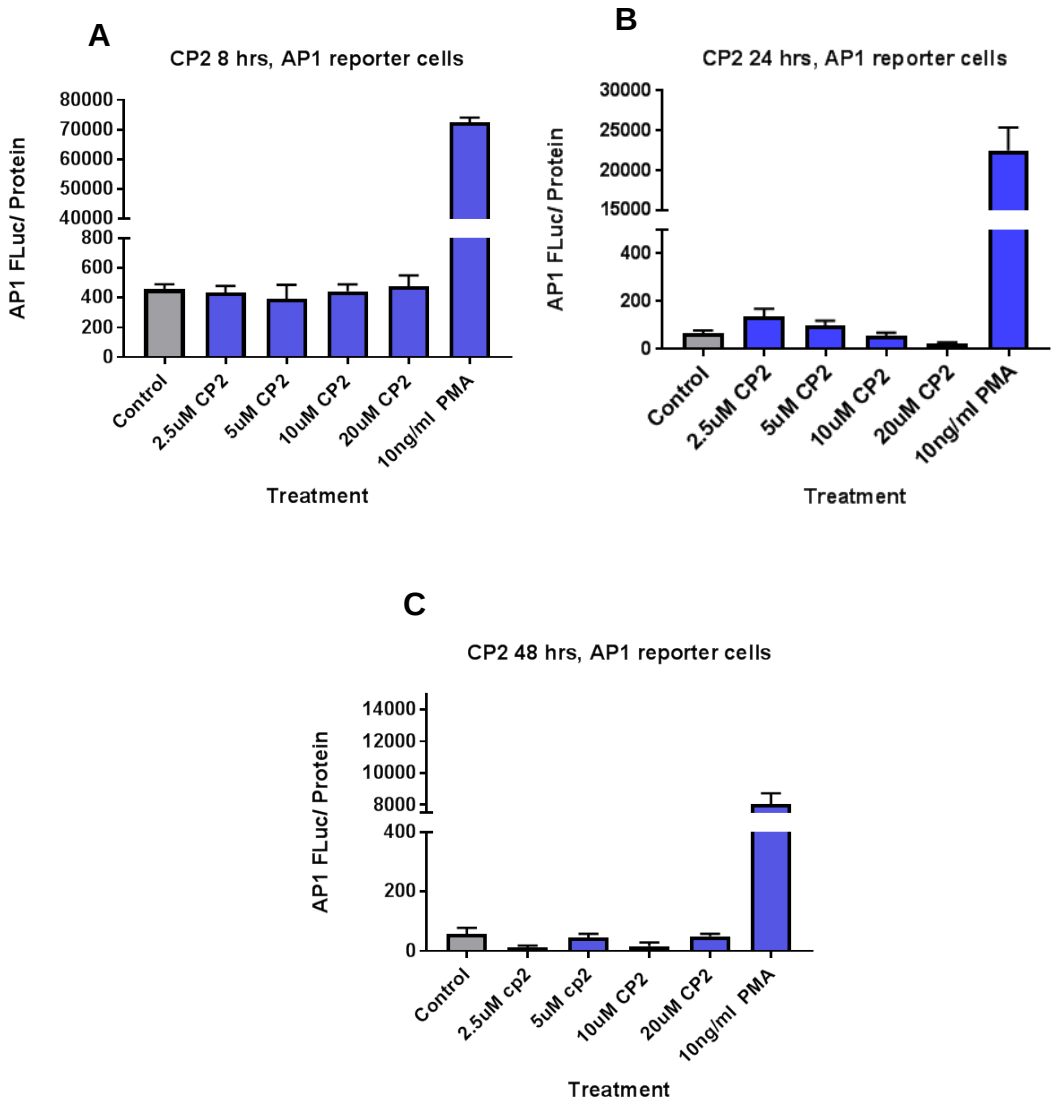

Figure 4.6. CP2 does not induce AP1 activation in HEK293 reporter cells.
AP1 activation was measured after 2.5 µM- 20 µM CP2 treatment for 8 (A), 24 (B) and 48 (C) hrs using the luciferase assay in AP1 HEK293 reporter cells. Luminescence data was normalized to the protein concentration. All the graphs shown are the representative of three independent experiments. Data is presented as mean +/- SE of triplicates; t-test is used for the statistics, **, $p < 0.01$;***, $p < 0.005$

4.3. CP2 treatment induces mild ROS production, which is consistent with mitohormetic mechanism

Since it is known that CP2 leads to a partial inhibition of respiration and mild ROS production at concentrations below 20 µM in isolated mitochondria (Figure 1.9), I examined if CP2 induces ROS production in HEPG2 reporter cells. For the measurement of ROS in reporter cells, 0.5 million cells were seeded in 6 well plate in rich MEM media and incubated overnight. Next day, cells were treated with 20 µM CP2, a concentration that is non-toxic to cells (Figure 1.8) but leads to the NRF2 activation (Figure 4.4). ROS generation was detected using mitosox, a dye that shifts fluorescent wavelength upon oxidizing by ROS as shown in Figure 4.7. Cells were incubated with 5 µM mitosox in HBSS buffer for 10 min at 37°C, followed by 20 µM CP2 treatment for 90 min at 37°C. After incubation with CP2, cells were trypsinised, collected in PBS + 5% FBS solution, and analyzed by flow cytometry at 488 nM excitation/580 nM emission wavelength. Results were analyzed using Cell quest software (BD biosciences). I found that non-toxic concentration of CP2 leads to a generation of ROS. As a control, I pre-incubated cells with 2 mM of NAC ((N-acetyl-L-cysteine, a known ROS scavenger) for 1 hour before treatment with mitosox. I found that NAC treatment abolished ROS generation (Figure 4.8). This experiment demonstrates that CP2 leads to a production of sub-lethal levels of ROS in HEPG2 reporter cells, which could lead to the activation of NRF2/ARE pathway via mitohormesis without inducing any cellular toxicity.

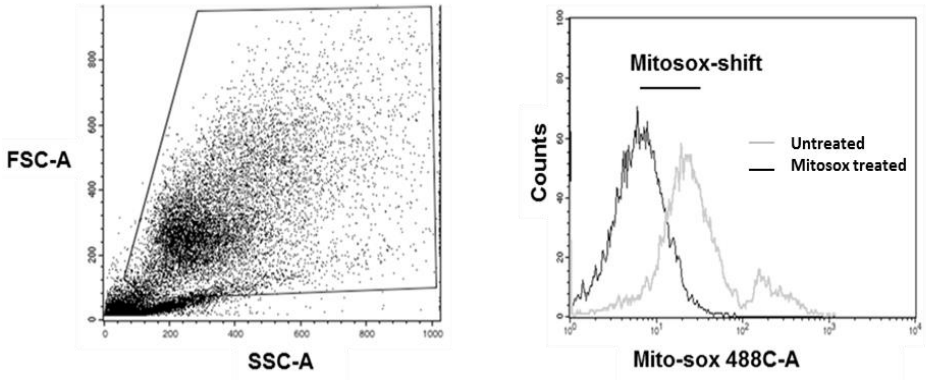

Figure 4.7. Demonstration of FACS analysis using mitosox.
Dot plot shows selection of the population of cells based on forward and side scattering and histogram shows the comparison between mitosox treated and untreated samples as controls.

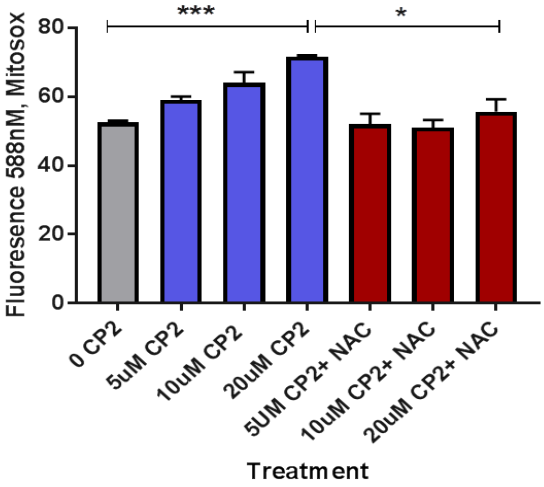

Figure 4.8. CP2 leads to a production of ROS in HEPG2 ARE reporter cells.
ROS generation was measured in HEPG2 ARE reporter cells using mitosox and flow cytometry. Graph is the representative of two independent experiments. Data is represented as the mean +/- SE of duplicates; t-test is used for the statistics, *, $p<0.05$, ***, $p < 0.005$.

4.4. CP2 does not induce a sustainable ROS activation, which is consistent with the mitohormetic mechanism

I further determined whether CP2-induced activation of ROS is consistent with the mitohormetic mechanism by comparing the kinetics of ROS production induced by CP2 vs. antimycin in HEPG2 ARE reporter cells. Antimycin, a known complex III inhibitor, generates high levels of ROS leading to cell death [64]. Unlike the last experiment where mitosox treatment was done prior to CP2 treatment, HEPG2 ARE reporter cells were first treated with 20 µM or 50 µM of CP2 for 5, 15, 45 min and 1 hour at 37°C. Cells were then incubated with 5 µM mitosox in HBSS for 10 min at 37°C. After incubation, cells were trypsinised, collected in PBS + 5% FBS, and analyzed by flow cytometry at 488 nM excitation/580 nM emission wavelength. Results were analyzed using Cell quest software (BD biosciences). I observed a very different kinetics of ROS production in cells treated with CP2 vs. cells treated with antimycin (Figure 4.9). Acute CP2 treatment produced transient increase in ROS levels with a rapid decay consistent with the signature of ROS production involved in mitohormesis [42]. However, levels of ROS induced by antimycin treatment continued to progressively increase over a prolong period of time, which eventually results in cell death (Figure 4.9)

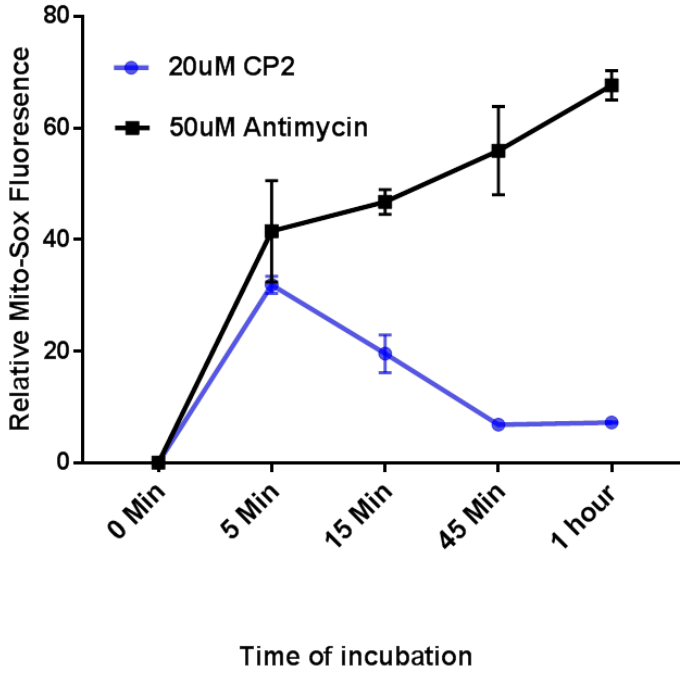

Figure 4.9. CP2 generates a transient increase in ROS production in HEPG2 ARE reporter cells followed by a decay compared to a sustained ROS production in antimycin-treated cells.
HEPG2 ARE reporter cells were treated with CP2 (20 µM) or antimycin (50 µM) for indicated time points followed by incubation with mitosox (5 µM) for 10 min, and cells were sorted based on fluorescence 488 excitation and 580 emission. Data was background corrected and each data point represents mean of three independent measurements and bars denote standard error.

4.5. Treatment with antioxidants abrogates CP2-induced activation of NRF2 in HEPG2 ARE reporter cells

In order to confirm that generation of ROS is essential for the CP2-induced NRF2 activation, I examined whether a pre-incubation with anti-oxidants that would sequester CP2-induced ROS and abolishes CP2 efficacy in HEPG2 reporter cells. HEPG2 reporter cells were pre-incubated with 0.5 - 1 mM of trolox or 2 mM of NAC for 1 hour. Cells were treated with 20 µM of CP2, and NRF2 activation was assayed 24 hrs later by measuring luminescence using the same experimental procedure as described in Figure 4.3. I found that trolox pre-treatment totally abolished the NRF2 activation, while NAC pre-treatment partially reduced the NRF2 activation by CP2 treatment. Difference in the activity of trolox and NAC is attributed to the fact that trolox is a direct ROS scavenger; however, NAC reduces cellular ROS by inducing synthesis of glutathione. This suggests that CP2-induced ROS production is essential for signaling involved in the NRF2 activation (Figure 4.10). This data provides further support for mitohormetic mechanism involved in the CP2-induced activation of NRF2/ARE pathway and protection against oxidative stress.

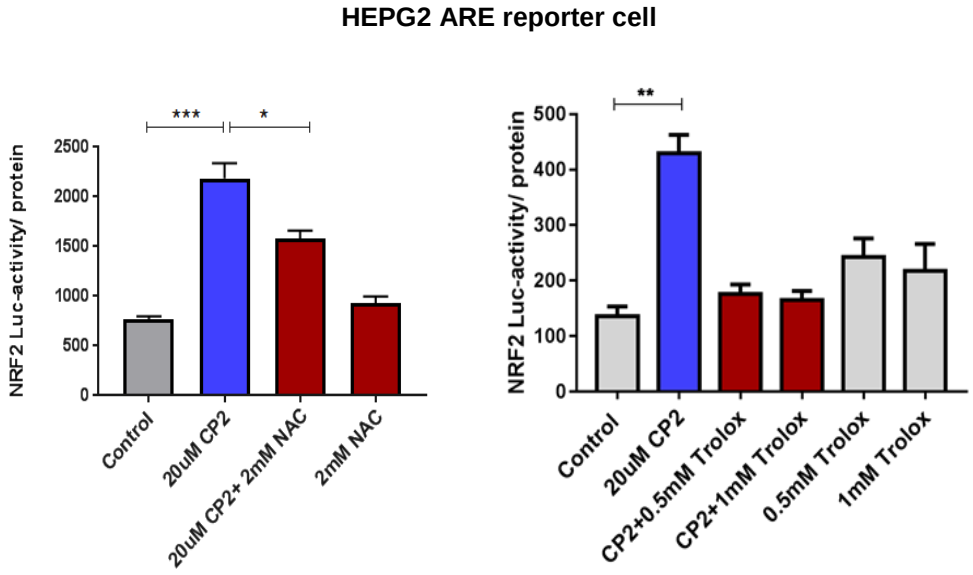

Figure 4.10. Anti-oxidant treatment abrogates CP2-induced NRF2 activation.
HEPG2 ARE reporter cells were pretreated with trolox or NAC, followed by 24-hours incubation with 20 µM CP2. Graphs represent two independent experiments. Data is represented as Mean +/- SE of triplicates; t-test was used for statistical analysis; *, $p < 0.05$, **, $p < 0.01$, ***, $p < 0.005$.

4.6. CP2 induces NRF2 activation *in vivo* in ARE reporter mice

My previous data generated in ARE reporter cells demonstrated that CP2 induces activation of NRF2/ARE pathway. I next validated whether CP2 induces NRF2 activation *in vivo* using ARE reporter mice [65]. The schematic diagram representing the generation of ARE reporter mice that express a heat stable human alkaline phosphatase (hPAP) gene fused with the NRF2 promoter sequence is shown in Figure 4.11. Male and female ARE reporter mice were treated with CP2 (25 mg/kg/day via gavage) for 4 days. Control mice were gavaged with vehicle. Mice were sacrificed; brain tissue was collected. Two to five mg of frozen hippocampus brain tissue was homogenized in 1mL TMNC buffer (50 mM Tris pH 7.5, 5 mM MgCl2, 100 mM NaCl, and 4% 3-((3-cholamidopropyl) dimethylammonio)-1-propanesulfonate (CHAPS). The homogenate was freeze-thawed, and 25 μL was added to a white-walled 96 well plate and mixed with 75 μL of 200 mM diethanolamine (DEA) buffers. Plates were incubated for 20 min at 65°C to inhibit endogenous phosphatases. Following the addition of 100 μL of substrate solution [2X CSPD (Applied Biosystems, catalog# T2041), 2X Emerald reagent (Applied Biosystems, catalog# T2115), 5 mM MgCl2, and 150 mM DEA] and incubation in the dark for 20 min at room temperature, luminescence was measured using a microplate luminometer (Berthold Detection Systems, Pforzheim, Germany) with one second integration time. Luminescence values were normalized to protein concentration measured using bicinchoninic acid protein assay (Bio-Rad, catalog# 500012). ARE-hPAP activity was expressed as relative luminescence units (RLU) per

mg of protein. I found that CP2 treatment induces NRF2 activation in ARE reporter mice compared to vehicle-treated mice (Figure 4.13). These data further confirmed that CP2 induces transcriptional activation of the ARE pathway *in vivo*.

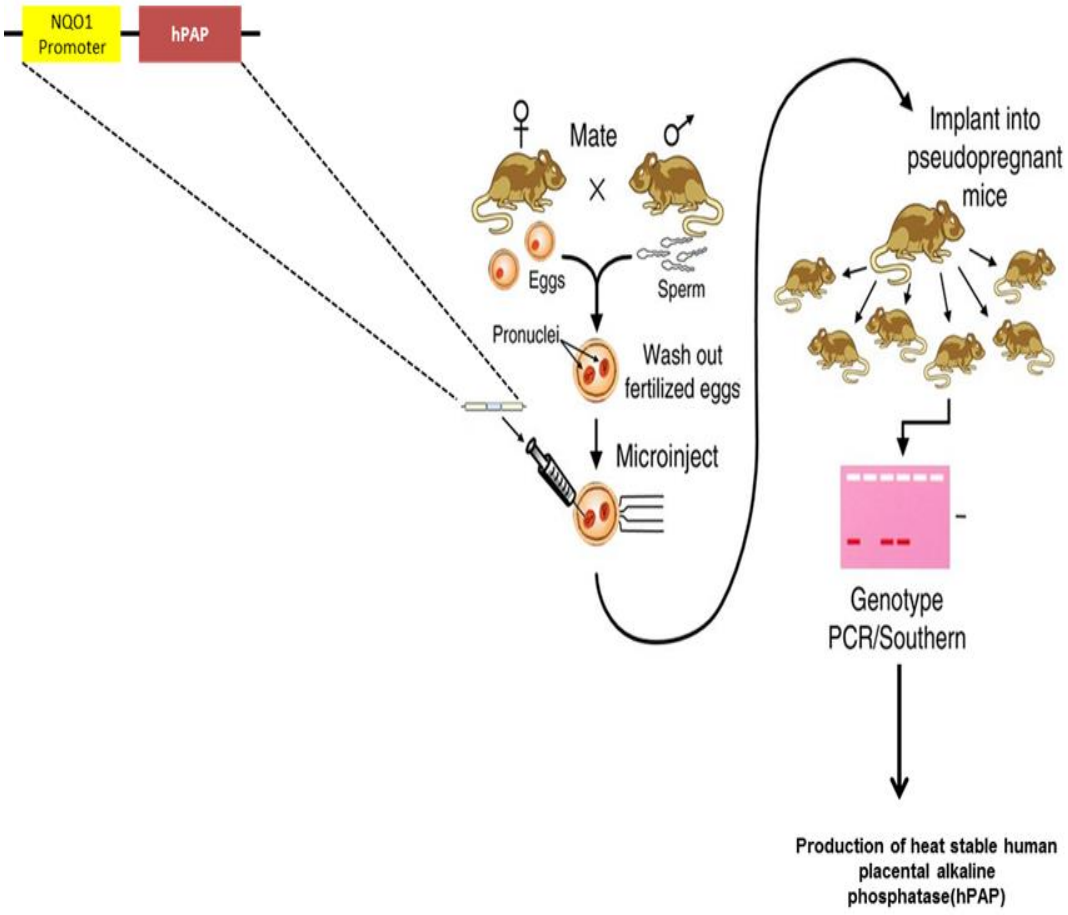

Figure 4.11. Generation of the ARE reporter mice.

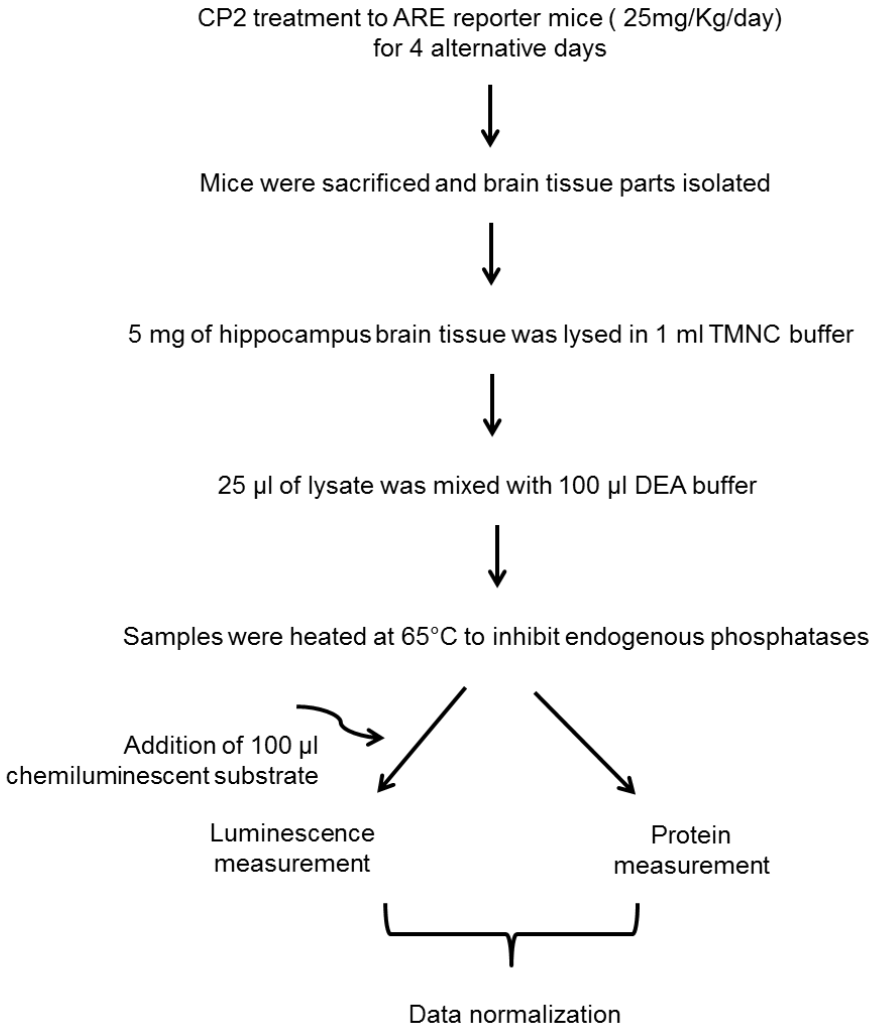

Figure 4.12. Schematic experimental procedure for measurement of hPAP activity in the brain tissue of ARE reporter mice treated with CP2.

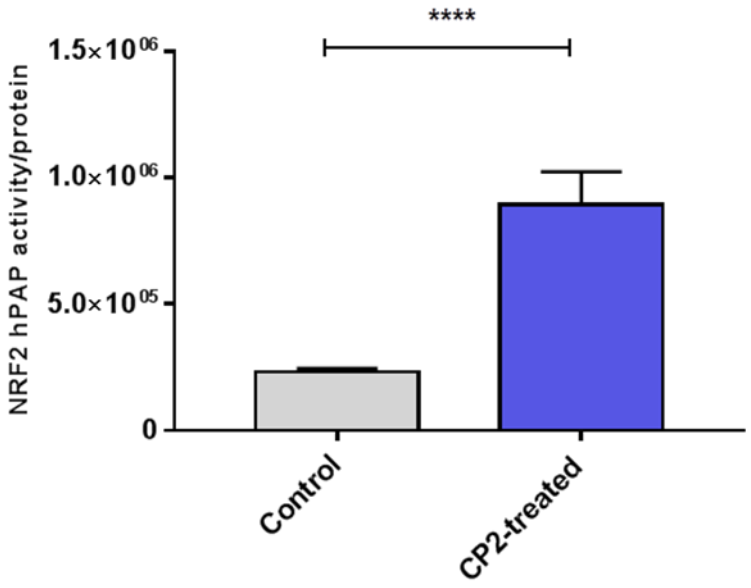

Figure 4.13. CP2 induces NRF2 activation *in vivo* in ARE reporter mice.
The activity of hPAP was measured by treating brain lysates with chemiluminescent alkaline phosphatase substrate. Data was normalized using protein concentration. N=4 for control mice and n = 2 for CP2-treated mice. Data is presented as Mean +/- SE of triplicates; results were analyzed using t-test. ****, $p < 0.001$.

4.7. CP2 protects against oxidative stress in Drosophila via NRF2 activation

To demonstrate that CP2 protects against oxidative stress via NRF2 activation, I employed the Drosophila model systems. Drosophila shares 70% of the genes that cause diseases in humans, and those genes can be easily modified for experiments to better understand any given molecular mechanism. The short lifespan and growth time to maturity make Drosophila an ideal model for performing survival experiments [66]. To examine the effect of CP2 treatment on protection against oxidative stress, I divided Drosophila into 2 groups consisting of 40 animals. The first group was treated with 2% hydrogen peroxide (H_2O_2) in 10% of sucrose solution. The second group was treated with 2% H_2O_2 and CP2 (25 mg/kg/day) in 10% of sucrose solution. The CP2 concentration was similar to the concentrations utilized in the previous studies demonstrating neuroprotection in mice [62]. I found that flies treated with CP2 survived longer compared to vehicle-treated files suggesting that CP2-induced protection against oxidative stress is conserved in Drosophila (Figure 4.14). Next, I examined whether NRF2 is required for oxidative stress protection in Drosophila by generating NRF2-RNAi files with reduced expression of NRF2 using GAL4-UAS system as explained in the Figure 4.15. For the generation of NRF2-RNAi files elav Gal4 female virgin were separated, these files express GAL4 transcription factor with elav promoter, which is specific for gene expression in the brain. Virgin files were crossed with male files having UAS (GAL4 DNA binding site) upstream of sequence for NRF2 RNAi or attp2 RNAi (genetic background control). After strain generation, experiment with these knockdown

strains was done within 21 days. Knockdown of NRF2 was confirmed by qPCR from the RNA isolated from files head (Figure 4.16). Survival studies were done in NRF2 RNAi flies as described previously. Consistent with our previous observations, the protection against oxidative stress was lost in Drosophila when NRF2 was knocked down further confirming that NRF2 is the key mediator of the CP2-induced mechanism of oxidative stress protection (Figure 4.17).

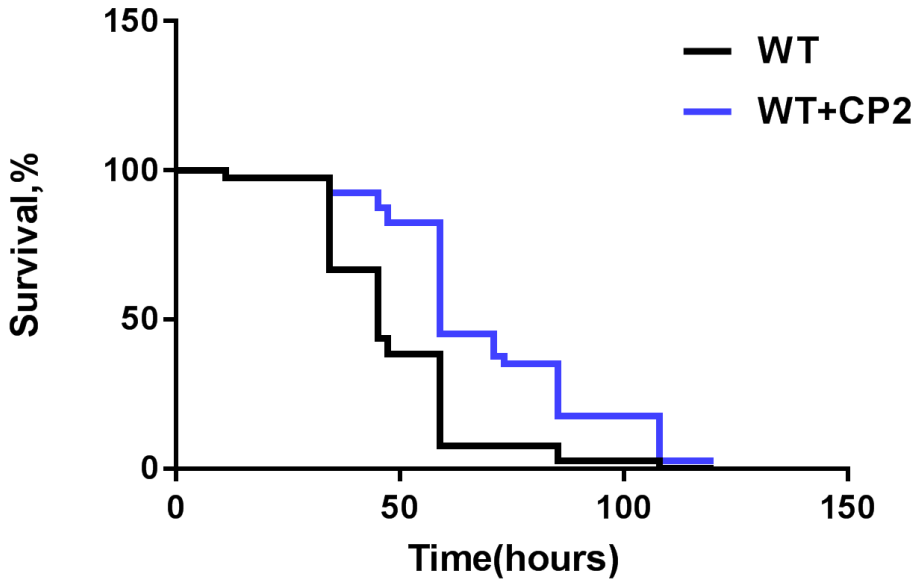

Figure 4.14. CP2 promotes the survival of Drosophila treated with 2% H_2O_2.
Graph represents three independent experiments each including 40 files.

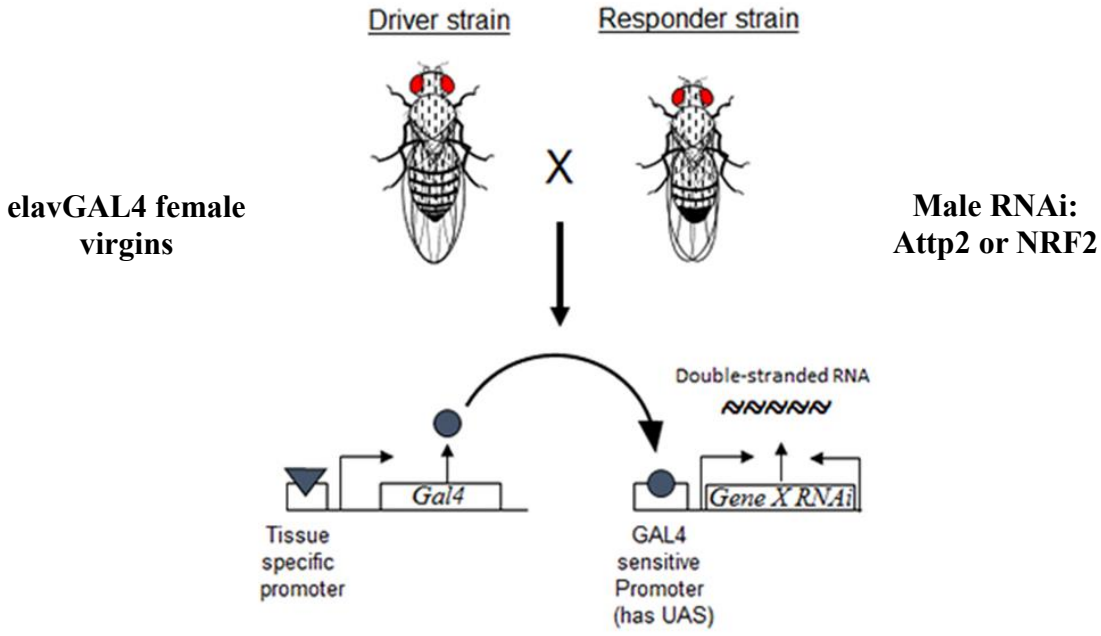

Figure 4.15. Diagram demonstrating the generation of RNAi Drosophila strain using UAS-GAL4 system.

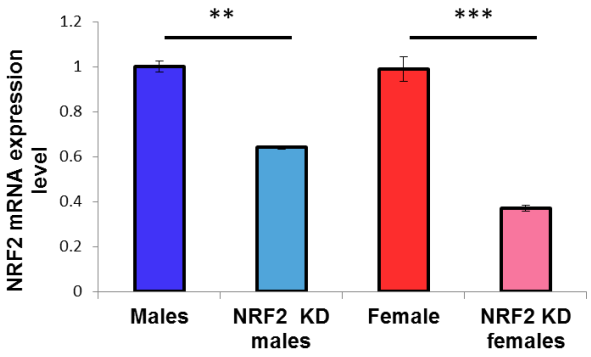

Figure 4.16. Confirmation of NRF2 expression in NRF2-RNAi Drosophila strain. mRNA level of NRF2 in Drosophila was measured in WT males and females files compared to NRF2-RNAi (KD) using one step qPCR SYGR kit. RP-49 was used as a housekeeping gene for data normalization. Data presented as Mean +/- SEM of triplicates. T-test was used for statistical analysis, **, $p < 0.01$, ***, $p<0.005$.

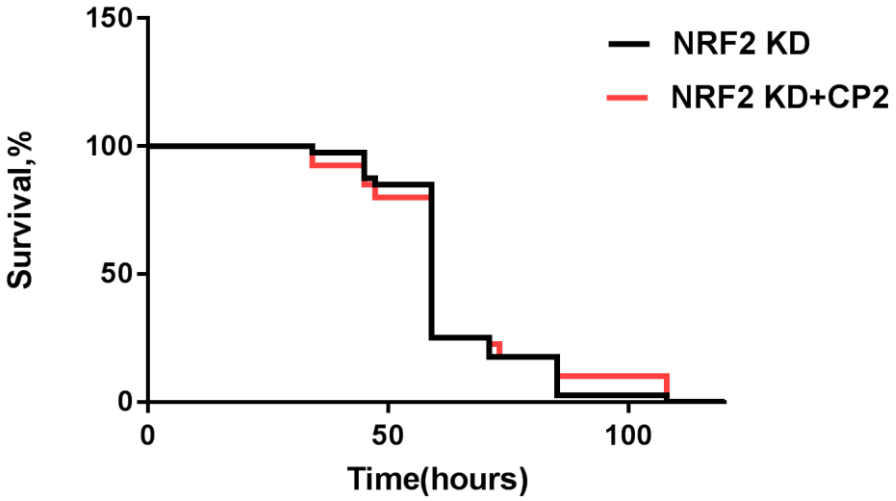

Figure 4.17. RNAi-mediated knockdown of NRF2 abrogates CP2-induced survival of Drosophila treated with 2% H_2O_2.
Graph represents three independent experiments each including 40 files.

4.8. CP2 protects against oxidative stress in wild-type mice fed with a high fat diet

Consumption of a high fat diet (HFD) negatively impacts metabolism by altering the substrate utilization pathways and leading to extensive oxidative damage, cognitive impairment and increased mortality [67, 68]. Specifically, studies have implicated that impaired NRF2 signaling and increased oxidative stress as mechanisms underlying HFD-induced decline in cognitive performance in the aged brain [69]. Interestingly it was found that mice on a HFD+CP2 showed a significantly greater survival rate and the lack of cognitive of behavior phenotype compared to the HFD group (Figure 1.8). All animals in HFD group developed multiple tumors confirmed during the postmortem

tissue examination while none of the animals in HFD+CP2 group developed tumors. To validate that CP2 protection was due to the reduced oxidative damage, I measured level of lipid peroxidation in the brain tissue collected from both cohorts of mice. Lipid peroxidation is caused by oxidative degradation of lipids. In this process, free radicals take electrons from lipids (generally located in membranes), resulting in cell damage. Quantification of lipid peroxidation is one the classical way to assess oxidative stress in pathophysiological processes. Lipid peroxidation forms reactive aldehydes such as malondialdehyde (MDA) and 4-hydroxynonenal (4- HNE) as natural bi-products. I measured the end product of lipid peroxidation, MDA, which is one of the most widely accepted assays for determining the extent of the oxidative damage. Using MDA standard provided in the kit, I found linear dose dependence between MDA concentration and absorbance values, which was used for the quantification of MDA in brain lysate samples (Figure 4.19). I found that CP2-treated HFD mice showed significantly lower lipid peroxidation compared to HFD group further validating that CP2 reduced oxidative damage *in vivo* promoting the survival (Figure 4.20).

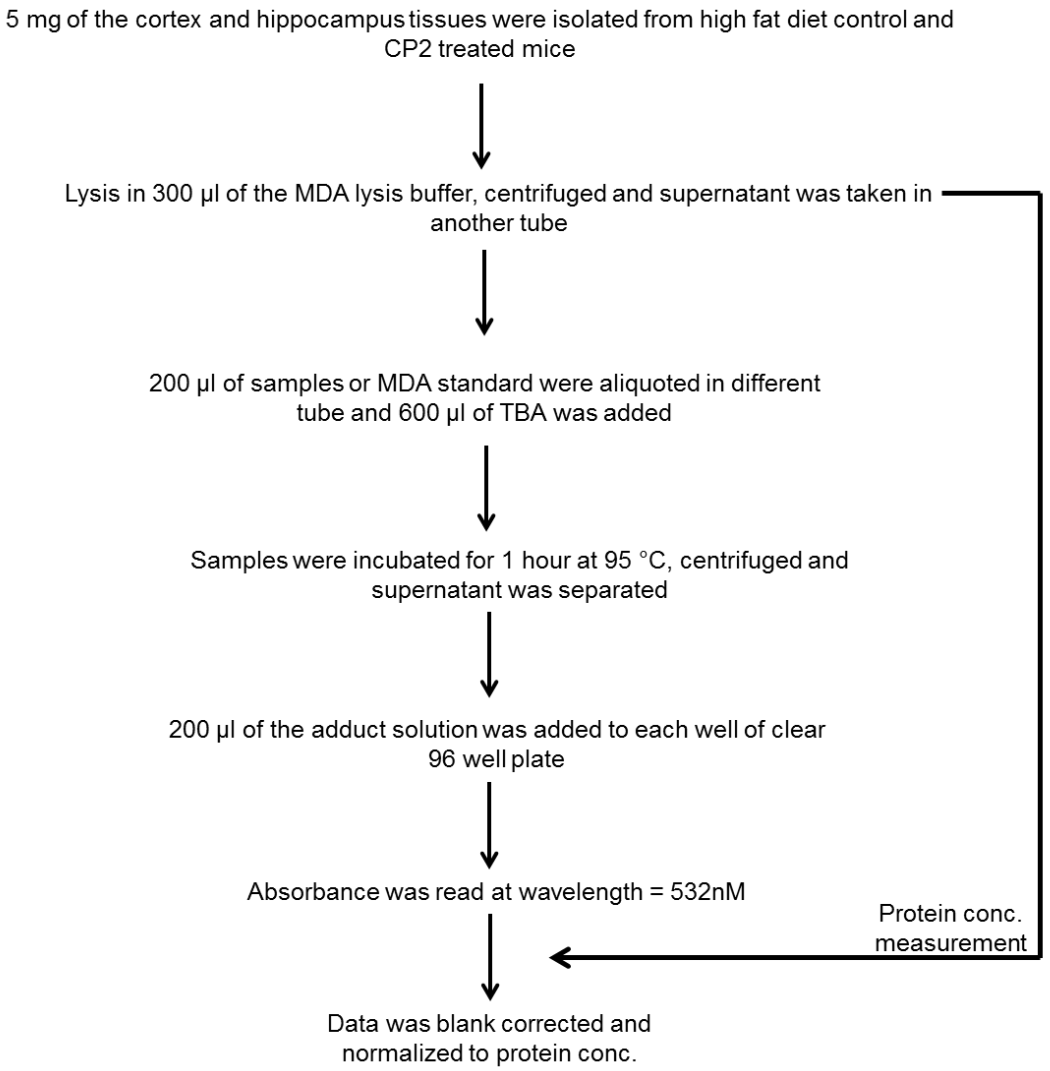

Figure 4.18. Schematic representation for quantification of MDA in mouse brain tissue isolated from a high fat diet mouse treated with CP2.

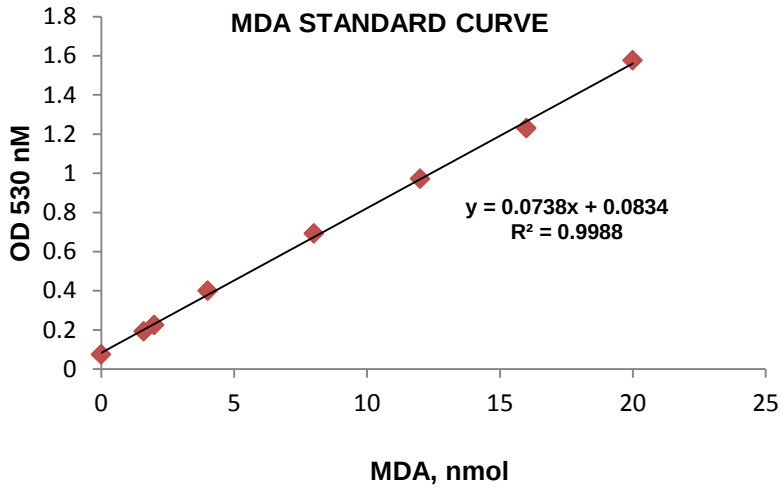

Figure 4.19. Standard curve of MDA

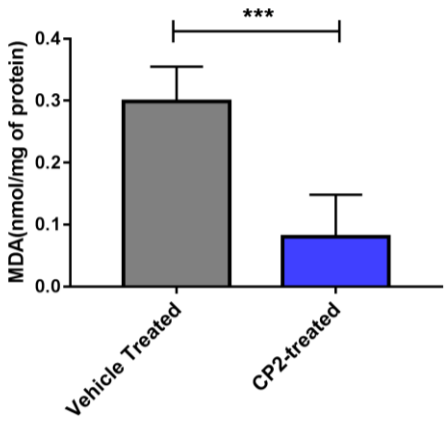

Figure 4.20. CP2 treatment reduces the level of lipid peroxidation in mice fed with a HFD.

Lipid peroxidation was compared in the hippocampus/cortex brain tissue isolated from vehicle or CP2-treated mice (n = 5 for each group) fed with a HFD for a year by measuring the concentration of malondialdehyde (MDA), a bi-product of lipid peroxidation. MDA forms a calorimetric adduct with thiobarbituric acid (TBA). Samples were treated according to the instructions provided with the kit (Sigma# MAK085) and

absorbance was measured at 532 nm. All experiments were conducted in triplicates. Raw data was normalized per protein concentration. T-test was used for statistical analysis, ***, $p < 0.005$.

4.9. Culturing of neurons from embryonic mouse brain

In order to demonstrate the molecular mechanism of CP2-induced mitohormetic response in the context of AD, I will use primary neuronal cells from embryonic mouse brain. Primary neuronal cultures represent a powerful model system to study mechanisms during a pre-clinical disease development providing an excellent tool for disease modeling, and pharmacological and genetic manipulations against neurodegenerative diseases. Postmortem analysis of brain tissue from AD patients shows the degeneration of cortex and hippocampus areas of the brain [70]. Therefore, I will use cortical neuronal cultures for studying the mechanism of CP2-induced neuroprotection. Embryonic day 17 (E17) mouse cortical tissue is more difficult to isolate than similar rodent tissue due to the size of the sample for dissection. One of the major advantages of using embryonic brain is the presence of high proportion of neuronal cell population as compared to other cell types like astrocytes and glia. In the protocol described (Methods, 3.14), I use specific media designed for neuronal growth and careful dissection procedure of embryonic cortical tissue to optimize growth of healthy neurons while minimizing contamination with other cell types. A brief description of steps involved in primary cortical neuronal culture from mouse embryonic brain is shown in Figure 4.21.

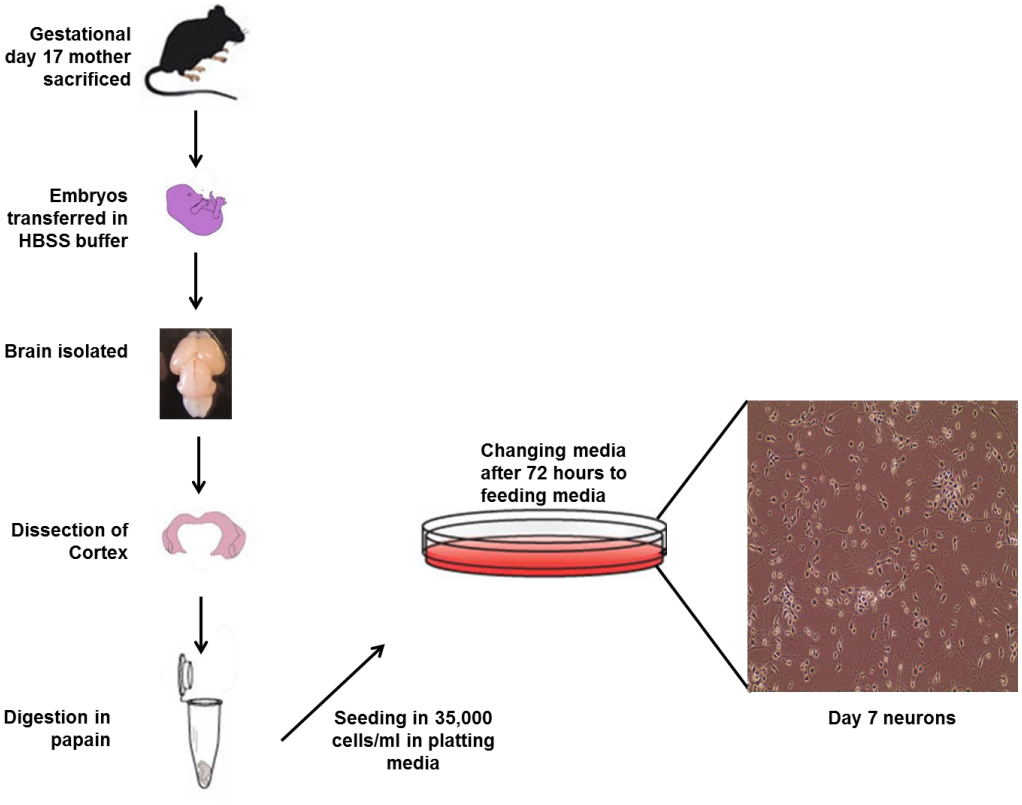

Figure 4.21. Schematic diagram of isolation of cortical neurons from E17 mouse brain.

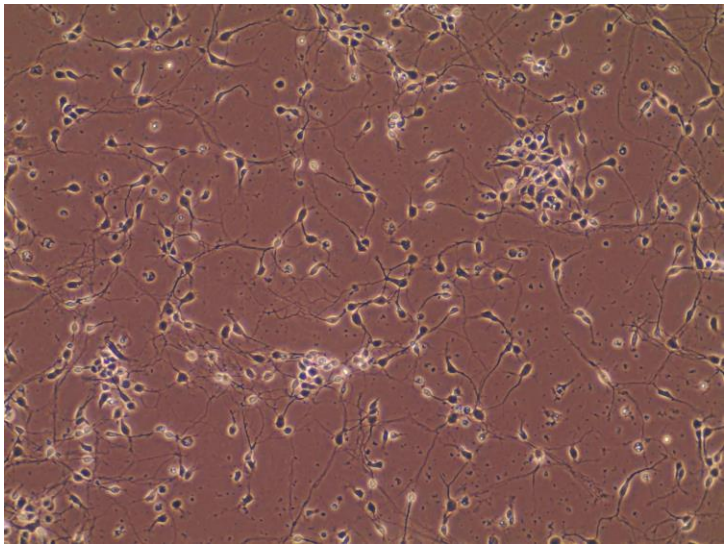

Figure 4.22. Bright field microscopy image of cortical neurons isolated from E17 mouse brain after 7 days in culture.
These neurons are fully developed based on the presence of well-developed neuronal processes. There is also no visible presence of glia cells and can be used for a variety of applications including immunocytochemistry, biochemistry, electrophysiology, calcium imaging, protein and/or DNA and RNA isolation. I performed this procedure three times using three individual time-pregnant mice together with Dr. Trushina. I also conducted three neuronal dissections and platings independently. The image represents results generated during my last independent neuronal plating. These cells were used by my colleagues to conduct bioenergetics studies required for the resubmission of the manuscript reviewed in *Neurobiology of Disease*.

I will use my ability to culture primary neurons (Figure 4.22) in my future studies to test whether CP2 treatment induces activation of NRF2/ARE pathway in these cells. NRF2 activation will be examined by monitoring its translocation to the nucleus using immunostaining. Further, I will also quantify the expression of anti-oxidant genes and the anti-oxidant enzymatic level using qPCR and enzyme-linked immunosorbent assay (ELISA) respectively in CP2-treated cortical primary neurons. ShRNA targeting NRF2 will be used to examine whether NRF2 plays a key role for CP2 induced protection

against oxidative stress in primary cortical neurons. All these experiments will further strengthen my knowledge about CP2-induced neuroprotection and will demonstrate activation of mitohormetic mechanism via CP2 in the cells directly affected in AD.

5. DISCUSSION

My work enhances the current understanding of the mito-nuclear communication and provides evidence that the beneficial reconfiguration of cellular metabolism and protective stress response could be triggered using pharmacological agents. My study dissected the molecular mechanism and signaling cascade activated by partial complex I inhibition using a small molecule CP2. Importantly, I demonstrated that CP2 activated the protection against oxidative stress via ROS-related mitohormetic mechanism. Through experiments done in isolated mitochondria and on cells, it was established that upon binding to complex I, CP2 generates a burst of sub-lethal levels of ROS. Consistent with the mitohormetic theory, low levels of ROS initiated signaling inducing activation of NRF2, upon CP2 treatment. CP2-induced NRF2 activation was abolished by anti-oxidant trolox and NAC validating that ROS generation and signaling is essential for the initiation of this mito-nuclear communication. However, together with ROS, this signaling cascade may be initiated by other factors such as MAP kinase, which also known to mediate mitohormesis [42]. Therefore, future studies will address the details of this CP2-mediated process. Through my experiments, I validated NRF2 activation via CP2 using multiple model systems including the ARE reporter cell lines, and the ARE reporter mice. Translational mechanism of CP2 was confirmed by a direct validation of target engagement, NRF2 activation and a protection against oxidative stress using mitochondria isolated from human postmortem brain, human neuronal cells, mouse neurons, Drosophila, and mice fed with a HFD. Reduction of the NRF2 expression in the

NRF2-RNAi Drosophila strain showed loss of protection against oxidative stress, confirming *in vivo* that NRF2 activation is the key mechanism for survival induced by CP2 under elevated oxidative stress conditions. Since oxidative stress is a main culprit of neurodegeneration observed in AD, demonstration that CP2 activates NRF2/ARE pathway extends our knowledge of the molecular mechanism involved in CP2-induced neuroprotection. Moreover, CP2 induced enhanced survival and reduced the extent of oxidative damage in WT ageing mice fed with a HFD, suggests that protective mechanisms induced by CP2 could alleviate oxidative damage associated with various disease conditions. These results provide a solid foundation to extend CP2 application to other human diseases associated with oxidative stress.

From the unpublished results in Dr. Trushina's lab, it is known that AMPK activation and mitohormesis induced by CP2 are two independent mechanisms. One of the interesting questions that remain to be addressed is what mechanism, AMPK-dependent or NRF2-dependent (Figure 5.1) plays the major role in neuroprotection depending on the stage of the disease. During the development of any disorder, levels of ROS associated with pathophysiological mechanisms could vary significantly from being low at pre-symptomatic stages to increasing significantly at symptomatic phase. Thus, it is possible that CP2-induced mechanism of neuroprotection via NRF2 activation may be functional only at the early stages since later in the disease progression increased oxidative stress could abolish the positive effect of CP2-ROS signaling. In this case, the

AMPK-dependent pathways activated by CP2 could become the key mechanism to provide neuroprotection (Figure 5.1).

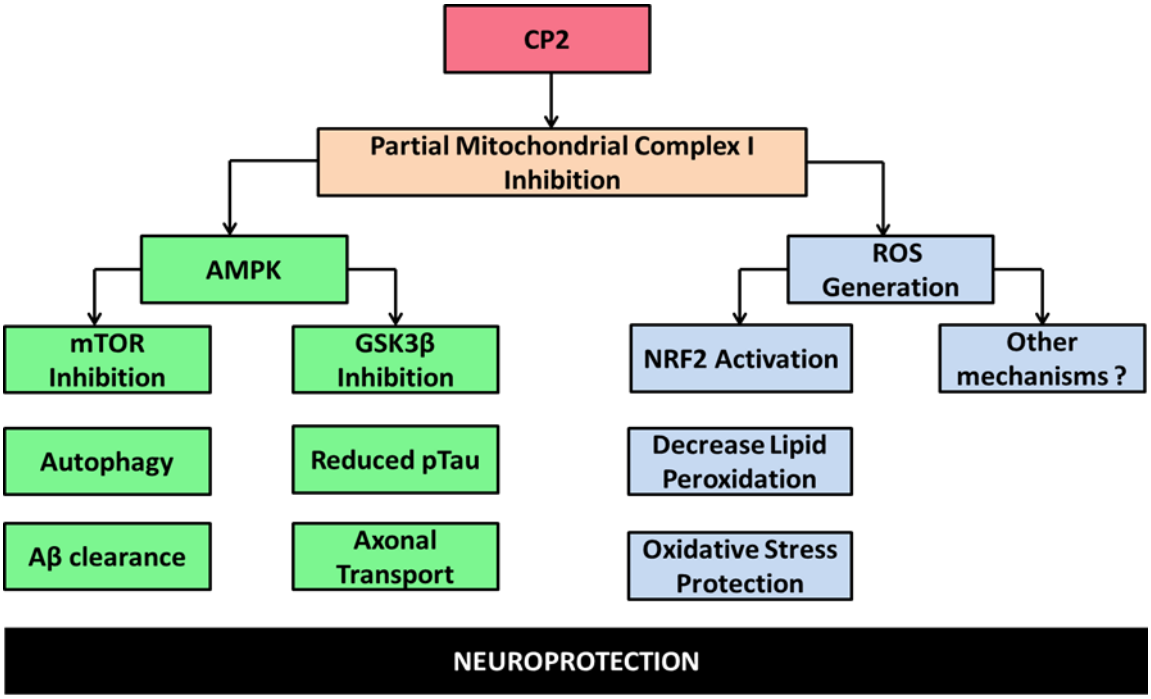

Figure 5.1. Molecular mechanism of CP2-induced neuroprotection.
In the previous study, we found that CP2 inhibits mitochondrial complex I leading to an increase in AMP/ATP ratio and activation of AMPK (green pathway). A downstream signaling cascade includes the reduction of GSK3β activity; activation of autophagy; reduction of levels of Aβ and pTau; restoration of axonal trafficking; increase in the levels of BDNF and synaptic proteins that ultimately contribute to neuroprotection. In my current study, I demonstrated that partial complex I inhibition also induces a sub-lethal production of ROS, which via mitohormetic mechanism activates the NRF2-ARE pathway. This transcriptional response could account for the observed reduction of markers of oxidative stress and prolonged health and lifespan in multiple *in vivo* models of human conditions that include oxidative stress.

While the application of partial complex I inhibitors appear to be controversial, a widely prescribed FDA approved drug, metformin, that is a partial complex I inhibitor is used to treat diabetes, supports the safety of this approach in humans, especially in the elderly population. The protective effect of metformin, in part, is also thought to be associated with ROS-induced mitohormetic mechanism [71]. However, compared to metformin, CP2 penetrates the blood brain barrier and appears not to have numerous molecular targets other than mitochondrial complex I. Thus, the development of safe and specific complex I inhibitors could provide therapeutic benefits against various diseases linked to oxidative stress including AD. Taken together, my results highlight differential and complex molecular mechanisms of CP2 that includes the NRF2-dependent stress response. Moreover, ROS generation and NRF2 activation are also the key mechanisms that are activated during exercise and caloric restriction, demonstrating that complex I inhibition via CP2 mimics these molecular signatures and their beneficial outcomes. Thus, it is feasible that CP2 could promote health and life span ultimately delaying the onset of age-related human diseases.

6. CONCLUSIONS

The study revealed that the NRF2 activation via partial complex I inhibition protects against oxidative stress in multiple model organisms. The protective effect of NRF2-ARE pathway activation has shown promising results for the treatment of multiple human conditions including AD and obesity [72-74]. Moreover, NRF2 acts as a transcriptional factor for more than 200 genes that not only participate in the expression of anti-oxidant enzymes but also in the promoting proteasomal and autophagic degradation, and anti- inflammatory response. Hence, I identified a novel CP2-induced mechanism that could be beneficial for a spectrum of chronic diseases linked to progressive oxidative stress, inflammation, and impaired autophagy. Based on my study, Dr. Trushina filed an invention disclosure entitled "Small Molecule Activators of the NRF2 Pathway", Mayo Case No. 2017-337.

REFERENCES

1. Karantzoulis, S. and J.E. Galvin, *Distinguishing Alzheimer's disease from other major forms of dementia.* Expert Review of Neurotherapeutics, 2011. **11**(11): p. 1579-1591.

2. Van Cauwenberghe, C., C. Van Broeckhoven, and K. Sleegers, *The genetic landscape of Alzheimer disease: Clinical implications and perspectives.* Genet Med, 2016. **18**(5): p. 421-430.

3. Dickson, D.W., *Neuropathological Diagnosis of Alzheime's disease: A perspective from longitudinal clinicopathological studies.* Neurobiology of Aging. **18**(4): p. S21-S26.

4. Tang, Y.-P. and E.S. Gershon, *Genetic studies in Alzheimer's disease.* Dialogues in Clinical Neuroscience, 2003. **5**(1): p. 17-26.

5. Selkoe, D.J., *Alzheimer's Disease: Genes, proteins, and therapy.* Physiological Reviews, 2001. **81**(2): p. 741-766.

6. William Rebeck, G., et al., *Apolipoprotein E in sporadic Alzheimer's disease: Allelic variation and receptor interactions.* Neuron, 1993. **11**(4): p. 575-580.

7. Barage, S.H. and K.D. Sonawane, *Amyloid cascade hypothesis: Pathogenesis and therapeutic strategies in Alzheimer's disease.* Neuropeptides, 2015. **52**(Supplement C): p. 1-18.

8. Masters, C.L., et al., *Amyloid plaque core protein in Alzheimer disease and Down syndrome.* Proceedings of the National Academy of Sciences of the United States of America, 1985. **82**(12): p. 4245-4249.

9. Kang, J., et al., *The precursor of Alzheimer's disease amyloid A4 protein resembles a cell-surface receptor*. Alzheimer Disease & Associated Disorders, 1987. **1**(3): p. 206-207.

10. Selkoe, D.J., *Biochemistry and molecular biology of Amyloid β-Protein and the mechanism of Alzheimer's disease*. Handbook of Clinical Neurology. 2008, Elsevier. p. 245-260.

11. Cummings, J.L., T. Morstorf, and K. Zhong, *Alzheimer's disease drug-development pipeline: few candidates, frequent failures.* Alzheimer's Research & Therapy, 2014. **6**(4): p. 37-37.

12. Swerdlow, R.H. and S.M. Khan, *A "mitochondrial cascade hypothesis" for sporadic Alzheimer's disease.* Medical Hypotheses, 2004. **63**(1): p. 8-20.

13. *Pathological correlates of late-onset dementia in a multicentre, community-based population in England and Wales.* The Lancet, 2001. **357**(9251): p. 169-175.

14. Khan, S.M., et al., *Alzheimer's disease cybrids replicate β-amyloid abnormalities through cell death pathways.* Annals of Neurology, 2000. **48**(2): p. 148-155.

15. Sheehan, J.P., et al., *Calcium homeostasis and reactive oxygen species production in cells transformed by mitochondria from individuals with sporadic Alzheimer's disease.* The Journal of Neuroscience, 1997. **17**(12): p. 4612.

16. Leuner, K., et al., *Mitochondrion-derived reactive oxygen species lead to enhanced Amyloid Beta formation.* Antioxidants & Redox Signaling, 2012. **16**(12): p. 1421-1433.

17. Tönnies, E. and E. Trushina, *Oxidative stress, synaptic dysfunction, and Alzheimer's disease.* Journal of Alzheimer's Disease, 2017. **57**(4): p. 1105-1121.

18. Guo, C., et al., *Oxidative stress, mitochondrial damage and neurodegenerative diseases.* Neural Regeneration Research, 2013. **8**(21): p. 2003-2014.

19. Halliwell, B., *Oxidative stress and neurodegeneration: where are we now?* Journal of Neurochemistry, 2006. **97**(6): p. 1634-1658.

20. Wang, X., et al., *Oxidative stress and mitochondrial dysfunction in Alzheimer's disease.* Biochimica et biophysica Acta, 2014. **1842**(8): p. 1240-1247.

21. Bratic, I. and A. Trifunovic, *mitochondrial energy metabolism and ageing.* Biochimica et Biophysica Acta (BBA) - Bioenergetics, 2010. **1797**(6): p. 961-967.

22. Persson, T., et al., *Oxidative stress in Alzheime's disease: Why did antioxidant therapy fail?* Oxidative Medicine and Cellular Longevity, 2014. **2014**: p. 11.

23. Ansari, M.A. and S.W. Scheff, *Oxidative stress in the progression of Alzheimer disease in the frontal cortex.* Journal of Neuropathology and Experimental Neurology, 2010. **69**(2): p. 155-167.

24. Nunomura, A., et al., *Oxidative damage is the earliest event in Alzheimer disease.* Journal of Neuropathology & Experimental Neurology, 2001. **60**(8): p. 759-767.

25. López-Otín, C., et al., *The hallmarks of aging.* Cell, 2013. **153**(6): p. 1194-1217.

26. Zahn, J.M. and S.K. Kim, *Systems biology of aging in four Species.* Current Opinion in Biotechnology, 2007. **18**(4): p. 355-359.

27. De Moura, M.B., L.S. dos Santos, and B. Van Houten, *Mitochondrial dysfunction in neurodegenerative diseases and cancer.* Environmental and Molecular Mutagenesis, 2010. **51**(5): p. 391-405.

28. Andreux, P.A., R.H. Houtkooper, and J. Auwerx, *Pharmacological approaches to restore mitochondrial function.* Nature Reviews Drug discovery, 2013. **12**(6): p. 465-483.

29. Mangialasche, F., et al., *Alzheimer's disease: Clinical trials and drug development.* The Lancet Neurology, 2010. **9**(7): p. 702-716.

30. Copeland, J.M., et al., *Extension of Drosophila life span by RNAi of the mitochondrial respiratory chain.* Current biology : CB, 2009. **19**(19): p. 1591-8.

31. Dillin, A., et al., *Rates of behavior and aging specified by mitochondrial function during development.* Science, 2002. **298**(5602): p. 2398.

32. Kim, Y. and H. Sun, *Functional genomic approach to identify novel genes involved in the regulation of oxidative stress resistance and animal lifespan.* Aging Cell, 2007. **6**(4): p. 489-503.

33. Lee, S.S., et al., *A systematic RNAi screen identifies a critical role for mitochondria in C. elegans longevity.* Nature Genetics, 2003. **33**(1): p. 40-8.

34. Baumgart, M., et al., *RNA-seq of the aging brain in the short-lived fish N. furzeri - conserved pathways and novel genes associated with neurogenesis.* Aging Cell, 2014. **13**(6): p. 965-74.

35. Baumgart, M., et al., *Longitudinal RNA-Seq analysis of vertebrate aging identifies mitochondrial complex I as a small-molecule-sensitive modifier of lifespan.* Cell Syst, 2016. **2**(2): p. 122-32.

36. Miwa, S., et al., *Low abundance of the matrix arm of complex I in mitochondria predicts longevity in mice.* Nature Communications, 2014. **5**: p. 3837.

37. Owen, M.R., E. Doran, and A.P. Halestrap, *Evidence that metformin exerts its anti-diabetic effects through inhibition of complex 1 of the mitochondrial respiratory chain.* Biochemical Journal, 2000. **348**(3): p. 607-614.

38. Guarente, L., *Mitochondria—A nexus for aging, calorie restriction, and sirtuins?* Cell, 2008. **132**(2): p. 171-176.

39. Merkwirth, C., et al., *Two conserved histone demethylases regulate mitochondrial stress-induced longevity.* Cell, 2016. **165**(5): p. 1209-1223.

40. Yun, J. and T. Finkel, *Mitohormesis.* Cell metabolism, 2014. **19**(5): p. 757-766.

41. Quiros, P.M., A. Mottis, and J. Auwerx, *Mitonuclear communication in homeostasis and stress.* Nat Rev Mol Cell Biol, 2016. **17**(4): p. 213-226.

42. Ristow, M. and K. Schmeisser, *Mitohormesis: Promoting health and lifespan by increased levels of Reactive Oxygen Species (ROS).* Dose-Response, 2014. **12**(2): p. 288-341.

43. Bailly, C., H. El-Maarouf-Bouteau, and F. Corbineau, *From intracellular signaling networks to cell death: The dual role of reactive oxygen species in seed physiology.* Comptes Rendus Biologies, 2008. **331**(10): p. 806-814.

44. Owusu-Ansah, E., W. Song, and N. Perrimon, *Muscle mitohormesis promotes longevity via systemic repression of insulin signaling.* Cell, 2013. **155**(3): p. 699-712.

45. Schmeisser, K., et al., *Role of sirtuins in lifespan regulation is linked to methylation of nicotinamide.* Nat Chem Biol, 2013. **9**(11): p. 693-700.

46. Schulz, T.J., et al., *Glucose restriction extends caenorhabditis elegans life span by inducing mitochondrial respiration and increasing oxidative stress.* Cell Metabolism, 2007. **6**(4): p. 280-293.

47. West, A.P., et al., *TLR signaling augments macrophage bactericidal activity through mitochondrial ROS.* Nature, 2011. **472**(7344): p. 476-480.

48. Chouchani, E.T., et al., *Mitochondrial ROS regulate thermogenic energy expenditure and sulfenylation of UCP1.* Nature, 2016. **532**(7597): p. 112-116.

49. Hayes, J.D. and A.T. Dinkova-Kostova, *The Nrf2 regulatory network provides an interface between redox and intermediary metabolism.* Trends in Biochemical Sciences, 2014. **39**(4): p. 199-218.

50. Tong Kit, I., et al., *Two-site substrate recognition model for the Keap1-Nrf2 system: a hinge and latch mechanism*, in *Biological Chemistry*. 2006. p. 1311.

51. Ma, Q., *Role of Nrf2 in oxidative stress and toxicity.* Annual Review of Pharmacology and Toxicology, 2013. **53**: p. 401-426.

52. Baird, L., et al., *Monitoring Keap1–Nrf2 interactions in single live cells.* Biotechnology Advances, 2014. **32**(6): p. 1133-1144.

53. Schmeisser, S., et al., *Neuronal ROS signaling rather than AMPK/sirtuin-mediated energy sensing links dietary restriction to lifespan extension.* Molecular Metabolism, 2013. **2**(2): p. 92-102.

54. Bryan, H.K., et al., *The Nrf2 cell defence pathway: Keap1-dependent and -independent mechanisms of regulation.* Biochemical Pharmacology, 2013. **85**(6): p. 705-717.

55. Kanninen, K., et al., *Nuclear factor erythroid 2-related factor 2 protects against beta amyloid.* Molecular and Cellular Neuroscience, 2008. **39**(3): p. 302-313.

56. Joshi, G., et al., *Increased Alzheimer's disease–like pathology in the APP/PS1ΔE9 mouse model lacking Nrf2 through modulation of autophagy.* Neurobiology of Aging, 2015. **36**(2): p. 664-679.

57. Lastres-Becker, I., et al., *Fractalkine activates NRF2/NFE2L2 and heme oxygenase 1 to restrain tauopathy-induced microgliosis.* Brain, 2014. **137**(1): p. 78-91.

58. Jo, C., et al., *Nrf2 reduces levels of phosphorylated tau protein by inducing autophagy adaptor protein NDP52.* Nature communications, 2014. **5**: p. 3496-3496.

59. Kobayashi, E.H., et al., *Nrf2 suppresses macrophage inflammatory response by blocking proinflammatory cytokine transcription.* 2016. **7**: p. 11624.

60. Li, W., et al., *Activation of Nrf2-antioxidant signaling attenuates NF-κB-inflammatory response and elicits apoptosis.* Biochemical Pharmacology, 2008. **76**(11): p. 1485-1489.

61. Gloire, G., S. Legrand-Poels, and J. Piette, *NF-κB activation by reactive oxygen species: Fifteen years later.* Biochemical Pharmacology, 2006. **72**(11): p. 1493-1505.

62. Zhang, L., et al., *Modulation of Mitochondrial Complex I Activity Averts Cognitive Decline in Multiple Animal Models of Familial Alzheimer's Disease.* EBioMedicine, 2015. **2**(4): p. 294-305.

63. Pang, Y.-P., *Low-mass molecular dynamics simulation: A simple and generic technique to enhance configurational sampling.* Biochemical and Biophysical Research Communications, 2014. **452**(3): p. 588-592.

64. Foster, J.G., et al., *Mitochondrial superoxide generation enhances P2X7R-Mediated Loss of Cell Surface CD62L on Naive Human CD4+ T Lymphocytes.* The Journal of Immunology, 2013. **190**(4): p. 1551-1559.

65. Johnson, D.A., et al., *Activation of the antioxidant response element in primary cortical neuronal cultures derived from transgenic reporter mice.* Journal of Neurochemistry, 2002. **81**(6): p. 1233-1241.

66. Podratz, J.L., et al., *Cisplatin induced mitochondrial DNA damage in dorsal Root ganglion neurons.* Neurobiology of Disease, 2011. **41**(3): p. 661-668.

67. Matsuzawa-Nagata, N., et al., *Increased oxidative stress precedes the onset of high-fat diet–induced insulin resistance and obesity.* Metabolism, 2008. **57**(8): p. 1071-1077.

68. Zhang, X., et al., *High dietary fat induces NADPH oxidase-associated oxidative stress and inflammation in rat cerebral cortex.* Experimental Neurology, 2005. **191**(2): p. 318-325.

69. Morrison, C.D., et al., *High fat diet increases hippocampal oxidative stress and cognitive impairment in aged mice: Implications for decreased Nrf2 signaling.* Journal of Neurochemistry, 2010. **114**(6): p. 1581-1589.

70. Schmitz, T.W., R. Nathan Spreng, and I. The Alzheimer's Disease Neuroimaging, *Basal forebrain degeneration precedes and predicts the cortical spread of Alzheimer's pathology,* Nature Communications,2016. **7**: p. 13249.

71. De Haes, W., et al., *Metformin promotes lifespan through mitohormesis via the peroxiredoxin PRDX-2.* Proceedings of the National Academy of Sciences, 2014. **111**(24): p. E2501-E2509.

72. Cuadrado, A., *NRF2 in neurodegenerative diseases.* Current Opinion in Toxicology, 2016. **1**(Supplement C): p. 46-53.

73. Ramsey, C.P., et al., *Expression of Nrf2 in Neurodegenerative Diseases.* Journal of Neuropathology and Experimental Neurology, 2007. **66**(1): p. 75-85.

74. Calkins, M.J., et al., *The Nrf2/ARE Pathway as a potential therapeutic target in neurodegenerative disease.* Antioxidants & Redox Signaling, 2009. **11**(3): p. 497-508.